

Geochemistry, Geophysics, Geosystems®



RESEARCH ARTICLE

10.1029/2022GC010726

Key Points:

- *Porites* corals grow normally with increased exposure to multiple metals over >1 year
- Skeletal partitioning variable within and between colonies and with seawater metal content
- Good agreement with previous work, especially for Pb across a large range of metal content

Supporting Information:

Supporting Information may be found in the online version of this article.

Correspondence to:

E. C. Hathorne,
ehathorne@geomar.de

Citation:

Schmidt, S., Hathorne, E. C., Schönfeld, J., Gosnell, K. J., & Garbe-Schönberg, D. (2024). Incorporation of dissolved heavy metals into the skeleton of *Porites* corals based on multi-element culturing experiments. *Geochemistry, Geophysics, Geosystems*, 25, e2022GC010726. <https://doi.org/10.1029/2022GC010726>

Received 3 OCT 2022

Accepted 20 AUG 2024




Author Contributions:

Conceptualization: Ed C. Hathorne, Joachim Schönfeld
Data curation: Sarina Schmidt
Formal analysis: Sarina Schmidt, Ed C. Hathorne, Kathleen J. Gosnell, Dieter Garbe-Schönberg
Investigation: Sarina Schmidt
Methodology: Sarina Schmidt, Ed C. Hathorne
Project administration: Ed C. Hathorne
Resources: Ed C. Hathorne, Joachim Schönfeld
Supervision: Ed C. Hathorne, Joachim Schönfeld
Writing – original draft: Sarina Schmidt

© 2024 The Author(s). Geochemistry, Geophysics, Geosystems published by Wiley Periodicals LLC on behalf of American Geophysical Union.

This is an open access article under the terms of the [Creative Commons Attribution License](#), which permits use, distribution and reproduction in any medium, provided the original work is properly cited.

Incorporation of Dissolved Heavy Metals Into the Skeleton of *Porites* Corals Based on Multi-Element Culturing Experiments

Sarina Schmidt¹, Ed C. Hathorne¹ , Joachim Schönfeld¹, Kathleen J. Gosnell¹ , and Dieter Garbe-Schönberg² 

¹GEOMAR Helmholtz Centre for Ocean Research Kiel, Kiel, Germany, ²Institute of Geosciences, Kiel University, Kiel, Germany

Abstract Anthropogenic activities increase the level of dissolved heavy metals in some tropical near-shore environments threatening reef ecosystems. The skeleton of stony corals like *Porites* species potentially provides a high-resolution geochemical archive for past heavy metal concentrations, with potentially century long records revealing baseline values before large-scale human disturbance. However, few data exist for heavy metal partitioning into coral skeleton aragonite. To address this, culturing experiments exposing *Porites lobata* and *Porites lichen* to a mixture of dissolved Cr, Mn, Ni, Cu, Zn, Ag, Cd, Sn, Hg, and Pb over a wide concentration range have been performed. Water samples were taken frequently to monitor changes in the heavy metal concentration. Laser ablation ICP-MS measurements of the coral aragonite revealed metal concentrations that were positively correlated with Cr, Mn, Ni, Zn, Ag, Cd, and Pb concentrations in seawater. The D_{TE} values for most metals appear dependent on the seawater metal content, approximating a power law, and therefore stabilize at higher seawater metal/Ca ratios. The partitioning of Pb into the coral skeleton is a notable exception, with D_{Pb} being stable around 2 to 1 across a large range of “natural” to highly polluted seawater Pb concentrations. This and the general agreement with partition coefficients estimated by previous work suggests that the reconstruction of the heavy metal concentration in seawater for ecosystem monitoring is possible. However, the high variability within and between coral colonies requires further study and suggests that multiple records from multiple coral colonies should be combined to obtain robust reconstructions.

1. Introduction

Modern tropical reefs undergo increasing degradation by natural and man-made factors such as global warming and associated extreme weather events, disease outbreaks, invasive coral predators, urban and agricultural runoff, ship anchoring, over-tourism and plastic pollution (e.g., Dar et al., 2018; Mieremet, 1997). These impacts impose stress on the corals and other organisms (e.g., Anthony, 1999; Corregé, 2006), and also introduce heavy metals to the oceans. Heavy metals occur naturally in the Earth's crust in generally low concentrations and geogenic sources include the chemical and physical weathering of rocks, leaching of soils and volcanic eruptions (Mansour et al., 2013). Heavy metals are defined here as elements with a density >7 g/cm³ (Venugopal & Luckey, 1975) and an atomic number beyond calcium (Bjerrum, 1936; Thornton, 1995). They can reach toxic levels if the ambient concentration exceeds a threshold, which can be caused by anthropogenic activities, for example, through emissions of industrial by-products (e.g., Nour, 2019; Weis, 2015). Heavy metals are highly persistent, not readily biodegradable and are thus concentrated along the food chain of aquatic organisms (Bosch et al., 2016; Diagonanolin et al., 2004; Liu et al., 2018; Santhanam, 2011; Sonone et al., 2020; Zhang & Gao, 2015). In the marine environment, metals occur as dissolved ions, molecular complexes, or bound to colloids and (suspended) sediments (Larocque & Rasmussen, 1998). The speciation of some metals like Mn is controlled by redox conditions and reactive oxygen species in the photic zone (e.g., Oldham et al., 2020) and in polluted coastal seawater up to around 50% of “dissolved” Cu, Cd, and Pb are present as colloids >1 kDa (Lu et al., 2019). Even in the truly dissolved phase (Ellwood, 2004), heavy metals are usually bound to inorganic (e.g., Byrne, 2002; Miller & Bruland, 1995) or organic ligands, the latter produced by marine organisms making seawater metal speciation complex and variable across regions (e.g., Hirose, 2006; Valverde et al., 2008). The toxicity of the metals depends on factors like concentration, synergistic-antagonist effects and chemical speciation.

Various marine organisms have been investigated as environmental indicators of heavy metal contamination and pollution (see Chapman, 2007 for a discussion on the definition of both). For example, plants like seaweed are

Writing – review & editing: Ed
C. Hathorne, Joachim Schönfeld, Kathleen
J. Gosnell, Dieter Garbe-Schönberg

capable of accumulating heavy metals (Arumugam et al., 2020; Besada et al., 2009; Davis et al., 2000), foraminifera have been used as bioindicators for heavy metal pollution in temperate and tropical seas (Frontalini & Coccioni, 2008; Li et al., 2021; Munsel et al., 2010; Oron et al., 2021; Titelboim et al., 2021), and marine sponges have been reported to bioaccumulate heavy metals (Batista et al., 2014; Cebrian et al., 2007; Rodríguez & Morales, 2020). Stony corals can be used as a tool for metal pollution monitoring because their skeletons exhibit clear growth bands, making excellent environmental archives accurately recording centennial to monthly physical and chemical environmental changes (Abdo et al., 2017; Al-Rousan et al., 2007; Chen et al., 2010; David, 2003; Nour & Nouh, 2020; Shen, 1996). Furthermore, corals can survive exposure to relatively high heavy metal concentrations (El-Sorogy et al., 2012; Readman et al., 1996). Corals have a long history as environmental archives based on the incorporation of different trace elements and metals into their skeleton (e.g., Amiel et al., 1973; Anu et al., 2007; Esslemont, 2000; Hanna & Muir, 1990; Jafarabadi et al., 2018; Kourandeh et al., 2021; Mohammed & Dar, 2010; Shen & Boyle, 1988) and Saha et al. (2016) provided a comprehensive review on the use of trace elements in coral skeletons. Metal-to-calcium ratios in coral skeletons have been used to investigate historic human activities and the long term impact of these activities on water quality throughout shallow tropical seas (e.g., Alibert et al., 2003; Carriquiry & Horta-Puga, 2010; Fleitmann et al., 2007; Jiang et al., 2020; Lewis et al., 2012; McCulloch et al., 2003; Nguyen et al., 2013; Prouty et al., 2010; Saha et al., 2016; Sowa et al., 2014). These studies demonstrate the ability of coral skeletons to record changing water quality due to land-use changes, industrialization, mining and deforestation.

The scleractinian coral genus *Porites* is globally distributed and has a simple growth structure. Different *Porites* species are found in the tropical Indo-Pacific Ocean (Kaczmarzsky & Richardson, 2007; Reyes-Bonilla, 1992; Tortolero-Langarica et al., 2017) including the Great Barrier Reef off eastern Australia (Lough et al., 1996; Wu et al., 2021) and in the Caribbean (Green et al., 2008; Lord et al., 2021). The growth rate of these massive stony corals allows measurements at sub-annual resolution as well as assembling continuous environmental archives covering hundreds of years (Clark et al., 2012; Kefu et al., 2001; Leonard et al., 2019; Schneider & Smith, 1982).

Most environmental pollution studies based on coral skeleton analysis were carried out using coral samples from field sites investigating heavy metal concentrations in naturally grown specimens in order to reconstruct past metal pollution (Barakat et al., 2015; Reichelt-Brushett & McOrist, 2003; Nour & Nouh, 2020, and references therein). Some studies have focussed on natural variations of metals like Mn and Cd in coral skeletons being related to climate modes such as ENSO (e.g., Carriquiry & Villaescusa, 2010; Linn et al., 1990; Sayani et al., 2021; Shen & Boyle, 1988), while others have examined corals from waters with many orders of magnitude higher seawater metal concentrations resulting from anthropogenic activities (Jiang et al., 2020). Studies reporting metal concentrations of seawater sampled near the corals are very rare and therefore large uncertainties surround the partitioning of metals into the coral aragonite skeleton (e.g., Jiang et al., 2020), especially when considering the spatial and temporal variability of metal concentrations observed around reef environments (e.g., Farkaš et al., 2018; Jiang et al., 2020; Kojima et al., 2022). To date, no culturing studies address the extent that changing seawater metal concentrations are incorporated into coral skeletons. Therefore, the main objective of this study was to investigate heavy metal incorporation into the skeleton of the stony corals *Porites lobata* and *Porites lichen*. Culturing experiments with a mixture of metals; chromium (Cr), manganese (Mn), nickel (Ni), copper (Cu), zinc (Zn), silver (Ag), cadmium (Cd), tin (Sn), mercury (Hg) and lead (Pb), were carried out over concentration ranges that cover situations in polluted and unpolluted near-shore environments today. The apparent partition coefficient (D_{TE}) between seawater and coral aragonite was constrained by relating analytical data of weekly to biweekly water samples to laser ablation ICP-MS measurements of the skeleton grown during culturing. The results refine the use of stony corals as a reliable monitoring tool to track anthropogenic footprints in presumably pristine tropical environments as well as in areas of high human impact.

2. Methods

2.1. Experimental Setup

Culturing experiments were configured with two experimental aquaria of identical dimensions and construction in an air-conditioned room. An additional large host aquarium was used for acclimation and nursery of commercially purchased corals. The host aquarium was described by Taubner et al. (2017). Four different coral colonies were acquired and species determined by genotyping. All colonies were divided into subcolonies and maintained in the host tank until the tissue had overgrown the cutting planes. Afterward, one sub-colony was

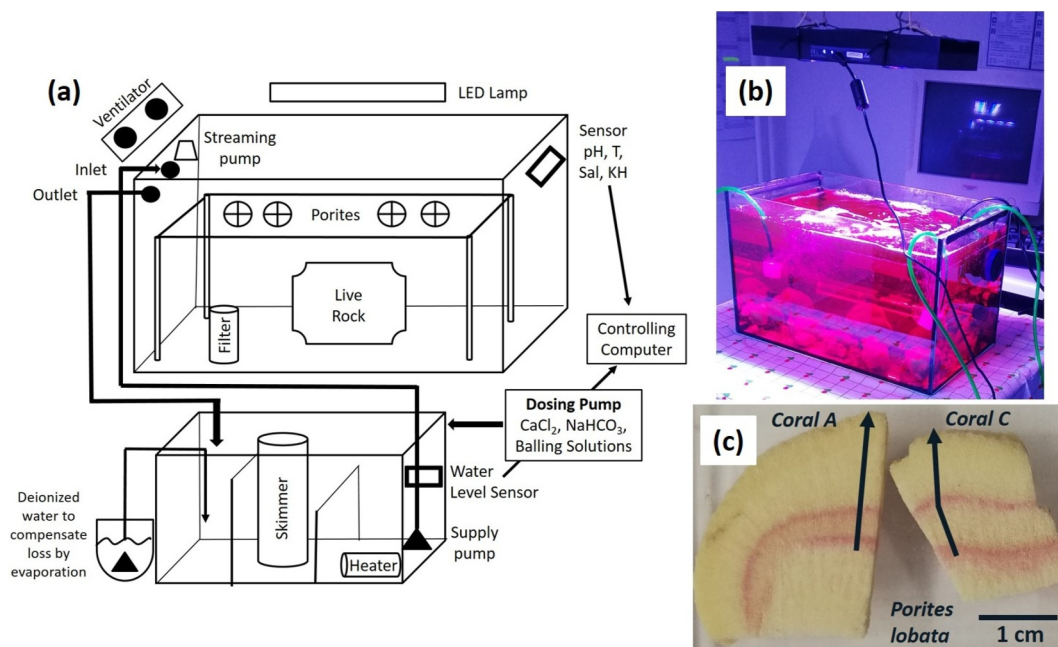


Figure 1. Schematic drawing of the culturing system (a), staining procedure with Alizarin Red S (b) and coral slices after culturing (c). Part c shows corals A and C. Furthermore, the course of the laser ablation line is indicated and the reddish staining lines are visible. Staining took place before Phase 0 and before Phase 1.

placed in each experimental tank and one was left in the host aquarium. The control aquarium remained unmodified while the trace metal concentration in the metal aquarium was elevated stepwise. The trace metal concentration in both tanks was monitored during the culturing period. Therefore, a direct comparison of a coral from the same colony growing in the same settings with only the heavy metal concentration of ambient seawater differing was possible. Although having only one experimental tank can be considered pseudo-replication (Hurlbert, 1984), we are not applying inferential statistics and having more experimental tanks would have been impractical for such a geochemical study. New growth was constrained by Alizarin Red S staining prior and during the experiment. After the experiment lasting more than 15 months, specimens were cut again and the growth was estimated from the stained bands and the time series of trace metal concentration in the coral skeleton was repeatedly measured by Laser ablation ICP-MS.

2.1.1. Culturing System

The two identical aquarium systems were built by Whitecorals, Korntal-Münchingen, Germany (Figure 1a). The design was adapted from earlier culturing facilities and professional aquaria (Allison et al., 2014; Taubner et al., 2017). Initial seawater was taken from the host aquarium. This system, which has been in operation since 2013, thus provided a complete ecosystem with adequate microbiology. The host aquarium water was mixed with North Sea water of 28 salinity units and the salinity was adjusted to 35 units by adding synthetic sea salt (Tropic Marin Pro-Reef®). Water exchanges of approximately 10 vol% were carried out every three to four weeks with artificial seawater during the complete culturing period. In addition, one L of water from the host tank was added to the experimental systems three times a week.

LED lamps (*Aquillumination Hydra 52 HD*) were used for illumination. The irradiation was set to 220–280 $\mu\text{mol photons m}^{-2} \text{s}^{-1}$ and a photoperiod of 10 hr dark-14 hr light with a dimming period of 1 hr before transition from dark to light in the morning and from light to dark in the evening. The color spectrum and intensity of the light were tuned to the values of illumination of the host tank, because the coral colonies were in good health and grew well with such a spectrum.

The main tank of each experimental aquarium had a water volume of 50 L and was equipped with a Tunze Turbelle nanostream 6045 streaming pump and an EHEIM aquaball 130 filter. Furthermore, an adjustable plastic grid made especially for the tank was installed, which made it possible to guarantee an optimal distance from the

lamps to the coral colonies. The water from the main tank flowed downwards via PVC tubing into a filter tank with three different chambers. Larger particles settled in the first chamber, while by mixing air and water in the second chamber, an Aqua Medic Evo 1000 protein skimmer removed hydrophilic proteins. The protein skimmer not only removed possible hydrophilic contaminants but also added air to the system, ensuring water oxygen saturation. Processed water was pumped back into the main tank by an EHEIM compact ON 300 pump with a flow rate of approximately 200 L per hour for the whole system. Water loss through evaporation was compensated by adding deionized water, which was automatically pumped into the third chamber of the filter tank when an optical water level sensor (GHL Level Sensor, Optolevel) registered a drop in water level. To maintain a constant water temperature at 25°C, a JBL Cooler 100 chiller on top of the main tank and an EHEIM thermocontrol 150 W heater in the filter tank were automatically controlled by a GHL Profilux computer.

Live rocks with high porosity were placed in the main tank to ensure a functional denitrification process, which is important for the water quality of the aquaria. Furthermore, snails and hermit crabs were inserted, which cleaned the aquarium from excessive algae and other leftover particles. The hermit crabs were fed 3 times a week with 1.5 pieces of NovoCrab food from JBL.

During coral growth, calcium and bicarbonate were consumed from seawater by the calcification of the coral skeleton. These were replenished by adding an adequate amount of two different stock solutions following the Balling Light method. Stock solution 1 consisted mainly of $\text{CaCl}_2 \cdot 2 \text{H}_2\text{O}$ and the Balling solutions 1 (high-purity water, $\text{BaCl}_2 \cdot 2 \text{H}_2\text{O}$, $\text{SrCl}_2 \cdot 6 \text{H}_2\text{O}$) and 2 (high-purity water, $\text{CoCl}_2 \cdot 6 \text{H}_2\text{O}$, $\text{MnSO}_4 \cdot \text{H}_2\text{O}$, $\text{CuSO}_4 \cdot 5 \text{H}_2\text{O}$, $\text{ZnSO}_4 \cdot 7 \text{H}_2\text{O}$, $\text{NiSO}_4 \cdot 6 \text{H}_2\text{O}$, $\text{FeSO}_4 \cdot 7 \text{H}_2\text{O}$, $\text{KCr}(\text{SO}_4)_2 \cdot 12 \text{H}_2\text{O}$). The main ingredient of stock solution 2 was NaHCO_3 mixed with Balling solution 3 (ultra-purity water, KI, NaF, $\text{Na}_2\text{B}_4\text{O}_7 \cdot 10 \text{H}_2\text{O}$). Both stock solutions were added four times a day using a Dupla Marin Dosing Pump P4 Smart. The total amount of the stock solution added per day varied due to changes in calcification rates between 16 and 24 mL.

Salinity, temperature and pH were measured two times an hour via GHL sensors placed in the main tank connected to a GHL Profilux 4 computer. Other water parameters such as calcium, magnesium, nitrate and phosphate concentrations, and carbonate hardness (which approximated seawater alkalinity) were monitored once a week. Phosphate and nitrate concentrations were measured using a custom Wasserpantcher photometer. All other tests were performed using JBL quick test strips. These quick tests were adequate for frequent measurements enabling the immediate reaction to changes in water quality.

2.1.2. Preparation for Culturing

Coral culturing was performed at GEOMAR from February 2019 to September 2020. Three colonies of *Porites* were purchased from different hobby aquarium retailers in Germany. After arrival, samples for DNA analyses of the coral tissue were taken to determine the species of the colonies. Genetic analyses and genotyping were performed by omics2view.consulting, Kiel, Germany. Sanger sequencing of cytochrome c oxidase subunit I mitochondrial genes (COI) and the nuclear ribosomal internal transcribed spacer region (ITS) was performed. The sequence was compared with GenBank data for species determination. Reference sequences of COI and the ITS from Forsman et al. (2009) were retrieved from NCBI (Sayers et al., 2009) and the program BLAST + v2.9.0 (Altschul et al., 1990) was used to find close relatives for the sequences. Maximum likelihood phylogenetic trees were calculated from multiple sequence alignments (produced with MAFFT v7.427, Katoh et al., 2002; Katoh & Standley, 2013) with IQ-TREE v1.6.10 (Nguyen et al., 2015).

Before colonies were inserted into the culture aquaria, they were kept in the host tank for several weeks to monitor their health and give them time to acclimatize to the new environment. These colonies were divided into three equal sub-colonies using a disinfected handsaw. Sub-colonies which were not able to stand on their own were glued with AQUA SCAPE FIX (Fauna Marin GmbH coral glue) to a breed disc holder. Sub-colony sizes varied according to the size of the mother colony and were between 5 and 10 cm in diameter. All colonies were maintained in the host tank for at least 2 months to ensure an adequate recovery after cutting. All colonies grew during that time and displayed polyp activity and a bright color.

The culturing aquaria underwent an initial acclimatization period lasting approximately 4 months. During this period, the biological parameters equilibrated (e.g., denitrification processes) and the accompanying organisms and corals were inserted stepwise. The first inhabitants were soft corals (*Capnella* sp.), snails and hermit crabs followed by different stony corals (*Pocillopora* sp., *Seriatopora* sp. and *Montipora* sp.). When these corals grew

Table 1

Heavy Metal Concentration in the Stock Solution, Target Concentration of These Metals in Each Phase in the Metal System and Salt Compounds

	Salt compound	Conc. mg L ⁻¹ stock	Target conc. in µg L ⁻¹				Actual conc. in µg L ⁻¹					Target/Actual (phase X – phase 0)			
			Phase 1	Phase 2	Phase 3	Phase 4	Phase 0	Phase 1	Phase 2	Phase 3	Phase 4	Phase 1	Phase 2	Phase 3	Phase 4
Chromium	CrCl ₃ * 6 H ₂ O	25	0.25	2.5	12.5	62.5	5.23	5.13	7.74	13.07	20.70	-0.39	1.00	0.63	0.25
Manganese	MnCl ₂ * 4 H ₂ O	40	0.4	4	20	100	2.38	4.36	4.71	16.34	49.85	4.95	0.58	0.70	0.47
Nickel	NiCl ₂ * 6 H ₂ O	5	0.05	0.5	2.5	12.5	1.15	0.87	1.55	9.37	24.65	-5.72	0.79	3.29	1.88
Copper	CuCl ₂ * 2 H ₂ O	2	0.02	0.2	1	5	1.93	1.22	1.26	2.89	3.86	-35.49	-3.35	0.96	0.39
Zinc	ZnCl ₂	50	0.5	5	25	125	0.71	0.99	4.99	39.88	98.04	0.58	0.86	1.57	0.78
Silver	AgNO ₃	3.5	0.04	0.4	2	10	0.006	0.023	0.048	0.61	2.23	0.44	0.11	0.30	0.22
Cadmium	CdCl ₂	4	0.1	1	5	25	0.02	0.07	1.00	11.28	31.55	0.46	0.98	2.25	1.26
Tin	SnCl ₂ * 2 H ₂ O	10	0.1	1	5	25	4.16	3.42	2.92	2.80	3.11	-7.33	-1.24	-0.27	-0.04
Mercury	HgCl ₂	0.04	0.004	0.04	0.2	1	0.58	1.53	7.40	52.18	314.09	0.24	0.17	0.26	0.31
Lead	PbCl ₂	10	0.1	1	5	25	0.03	0.06	0.46	3.37	7.45	0.38	0.43	0.67	0.30

Note. All salts used were p.a. (pro analysis) purity. For Hg Phase 0 is the mean of the control.

and showed a good vitality, the sub-colonies of *Porites* were inserted into the experimental tanks. Prior to this, the growth stage was marked. The sub-colonies were set into a smaller aquarium containing water with Alizarin Red S (~16 mg/L; 3,4-Dihydroxy-9,10-dioxo-2-anthracenesulfonic acid sodium salt, Sigma Aldrich; Figure 1) and left in there for approximately 8 hr for staining. In the presence of calcium, Alizarin Red S adsorbs to calcium and forms a pigment that is orange to red in color. Afterward, the corals were put back into the host tank to recover for approximately 1 week until they were inserted into the culturing aquaria.

2.1.3. Experimental Setup

The culturing period was divided into different phases. Phase 0 lasted for 19 weeks, Phase 1 to 3 took 10 weeks each and Phase 4 covered 13 weeks. One aquarium was used as the control, in that no metals were added to the water.

Sub-colonies from corals A through D were inserted into the metal and control systems. Phase 0 was an initial control phase without any extra-added metals in both systems. A second staining with Alizarin Red S was carried out after Phase 0 to mark the onset of the metal addition and to estimate the growth rate of the colonies (Figure 1). Beginning with Phase 1, the heavy metal concentration in the metal system was elevated stepwise by adding a certain amount of the stock solution (Phase 1 = 8.2 mL; Phase 2 = 82 mL, Phase 3 = 410 mL; Phase 4 = 2,050 mL; Table 1). For maintaining the heavy metal concentration during each culturing period as stable as possible, an aliquot (Phase 1 = 0.1 mL; Phase 2 = 1 mL, Phase 3 = 10 mL; Phase 4 = 100 mL) of the stock solution was added daily to counteract uptake of heavy metals by the corals and other organisms, or removal by adsorption on surfaces of the system, protein skimmer and filters. During every water exchange, the stock solution was added to maintain metal concentrations at levels targeted for each phase with seawater renewal.

The target concentration of each metal (see Table 1) was selected to cover a wide range of concentrations resembling conditions observed in polluted tropical areas, for example, Jakarta Bay (e.g., Williams et al., 2000). The concentrations were selected attempting not to reduce growth and normal metabolism. Therefore, the recommended threshold values provided by the Environmental Protection Agency, USA (EPA) were followed. Additionally, values from Reichelt-Brushett and Harrison (2005) addressing the effect of heavy metals on coral fertilization were taken into account. Baudouin and Scoppa (1974) further investigated the toxicity of heavy metals to zooplankton, which was also considered. This step-wise increased exposure to multiple metals simultaneously was meant to mimic real world conditions where multiple metals and pre-exposure are likely to occur. The heavy metal concentrations in the seawater during each phase were monitored by frequent water sampling. Temperature, pH and salinity were kept stable at 25.1 (±0.2) °C, 8.3 (±0.1) and 34.9 (±0.3) units, and at 25.1 (±0.2) °C, 8.2 (±0.1) and 34.8 (±0.2) units in the metal system and control system, respectively, over the entire culturing period.

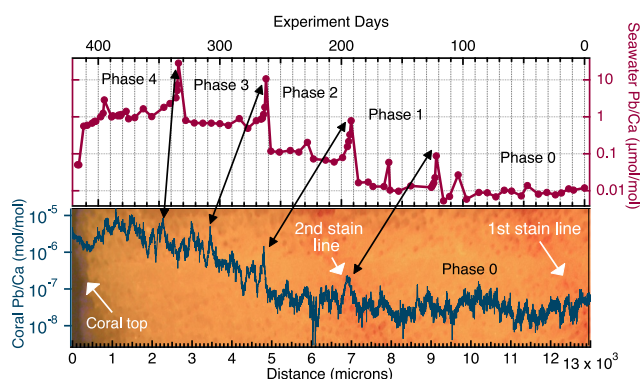


Figure 2. Example of a LA-ICP-MS line analysis of Pb/Ca across coral C from the metal system on top of color image taken under a binocular microscope of the laser analysis line showing the staining marks and coral top surface. The lower panel shows the seawater Pb/Ca over the experimental period for comparison.

2.2. Water Samples

To constrain the heavy metal concentration in the culturing medium, water samples were frequently taken from the metal and control systems (Table S1). Samples were taken using 25 mL syringes, filtered through a 0.2 μm PES syringe filter, and stored in HDPE bottles until analysis. Filters were flushed with >1 mL of sample water before taking each sample. The samples were acidified using distilled concentrated HCl (0.1 vol % of the sample volume) immediately after filtering. Mercury samples were further treated with bromine monochloride (BrCl) to ensure oxidation and release of all Hg species. All water samples were preconcentrated offline with a SeaFAST system (ESI, USA). For metals that cannot be preconcentrated by the resin used by the SeaFAST system (Cr, Ag and Sn), samples were diluted for ICP-MS analysis (Schmidt et al., 2022).

The element concentration in the seawater was determined by different techniques at GEOMAR (Mean values in Table 1, full data in Table S1 and shown in Figure 2). For major elements including Ca, inductively coupled plasma optical emission spectrometry (ICP-OES, Model VARIAN 720-ES)

was used on diluted samples. Frequent measurements of an IAPSO standard seawater revealed a precision expressed as the relative standard deviation (RSD %) of less than ±0.35% (mean Ca concentration IAPSO standard = $419.6 \pm 0.15 \text{ mg L}^{-1}$; reference Ca concentration based on the salinity of IAPSO Batch 161 = 423 mg L^{-1}). Cr, Mn, Ni, Cu, Zn, Ag, Cd, Sn and Pb concentrations were measured using an Agilent 7500ce quadrupole ICP-MS. The accuracy and precision derived from measurements of reference materials are given in Table S5 in Supporting Information S1. A Brooks Rand Model III Mercury system was used to analyze the total Hg content of samples following US EPA method 1631. Quality control of the Hg measurements revealed uncertainties smaller than 4.5% RSD for all analyses.

2.3. Coral Samples

After the culturing period, the corals were taken out of the experimental tanks and slices cut from each sub-colony (see Figure 1c). These slices were subsequently treated with sodium hypochlorite solution (NaClO, 13% Cl₂) for at least 24 hr to remove organic compounds. Afterward, the coral slices were rinsed with CaCO₃ equilibrated MilliQ >18.2 MΩ water to avoid dissolution of the aragonite and dried in an oven over night ($T < 40^\circ\text{C}$).

Micro-analytical analyses of the metal content in the coral skeleton were performed using Laser Ablation (LA)-ICP-MS at the Institute of Geosciences, Kiel University. A 193 nm ArF excimer GeoLasPro HD laser system (Coherent) with a large volume ablation cell (Zurich-type LDHCLAC, Fricker et al., 2011) and helium as the carrier gas was used. A small amount (14 mL min^{-1}) of H₂ was added to the helium to increase the sensitivity. Line scans were performed orthogonally to the growth direction of the coral from the periphery to the inner parts until passing the first staining line that marked the onset of the experiment (see Figure 1). Replicate lines were analyzed on different parts of the colonies. The laser and instrument settings are given in Table 2. Prior to every scan, a preablation pass was carried out to clean the cut surface of the coral skeleton. Before and after each line scan, the gas blank was measured for at least 30 s. These values were used as background intensities for the different masses monitored and subtracted from each ablation profile during the data reduction process. The isotope ⁴³Ca was used as an internal standard and the trace metal concentration of the samples was calibrated using the NIST SRM 612 glass reference material (Jochum et al., 2011). Because the NIST glass contains no mercury, the synthetic spiked carbonate MACS-3 (Jochum et al., 2019) was used for Hg calibration. Time resolved data were processed with the software Iolite (Version 4) to select integration and calculate element/Ca ratios using the “trace elements” data reduction scheme. The measured element/Ca ratios were converted to true element//Ca values using average factors obtained from the analyses of the NIST SRM 612 glass in each session. For Cu and Hg more than one isotope was analyzed. As the

Table 2
Laser and Instrument Settings

Laser	193 nm ArF excimer GeoLasPro
Energy density	10 J/cm ³
Spot size	120 μm, preablation 160 μm, glass 60 μm
Scan speed	50 μm/s
Pulse frequency	10 (Hz)
Isotopes monitored	²⁶ Mg, ²⁷ Al, ⁴³ Ca, ⁵² Cr, ⁵⁵ Mn, ⁶⁰ Ni, ⁶³ Cu, ⁶⁵ Cu, ⁶⁸ Zn, ⁸⁸ Sr, ¹⁰⁷ Ag, ¹¹¹ Cd, ¹¹⁴ Cd, ¹¹⁸ Sn, ²⁰¹ Hg, ²⁰² Hg and ²⁰⁸ Pb

values agreed well, the average value of both isotopes was used for further analysis. Carbonate matrix reference materials (coral JCP-1, giant clam JCT-1, limestone ECRM752-1; Inoue et al., 2004; Jochum et al., 2019) were analyzed in the form of nano-particle pellets (Garbe-Schönberg & Müller, 2014) for quality control. Spot analyses of these reference materials during the same analytical session gave a precision, expressed as one standard deviation in % (RSD %), generally less than 6% for TE/Ca values in the $\mu\text{mol/mol}$ range with the exception of Hg. Generally, good agreement with previous published values was obtained but there are few data for many of these elements available making accuracy difficult to properly assess. Here we provide TE/Ca values for these reference materials to help address this issue for future work (Table S6 in Supporting Information S1). The precision of line scan measurements as assessed by repeated line scans on the reference material nano-pellets JCP-1 and MACS-3, was better than 10% and 5% RSD, respectively, for all element/Ca ratios (Hg/Ca only for MACS-3). Statistical analysis of the data was performed using the program PAST (Hammer et al., 2001; Schmidt et al., 2022).

The partition coefficients (D_{TE}) of the different trace element/Ca ratios were calculated by using the corresponding molar ratios in the coral skeleton and seawater:

$$D_{\text{TE}} = (\text{TE}/\text{Ca})_{\text{coral}}/(\text{TE}/\text{Ca})_{\text{seawater}}$$

The calculation of growth rates for each sub-colony was primarily based on the stained lines that marked the onset of Phases 0 and 1. Within these constraints, the division between the following culturing phases was based on sudden and persistent elevations of metal concentrations in the coral skeleton observed in the LA-ICP-MS scans (Figure 2). These markers were available only in the metal system. The surface of the corals after termination of the experiment provided a third age control point available for all sub-colonies that survived the experiment.

A composite line was calculated individually for all colonies consisting of the laser ablation measurements along the major growth axis of the coral (coral A $n = 3$, coral B $n = 3$, coral C $n = 2$, coral D $n = 1$). No composite lines were constructed for the control coral samples and simple averages across the entire skeleton grown during the culturing period were used to compare with the seawater metal content of the control system. Laser ablation measurements along lines that deviated from the major growth axis of the coral were not included in the composite line as workers usually avoid off axis sampling to avoid known geochemical artifacts (e.g., Alibert & McCulloch, 1997; DeLong et al., 2013), and the data often exhibited much lower metal enrichment. Composite lines were aligned with QAnalyseries (Kotov & Pälke, 2018) and values resampled at an equal resolution to account for squeezing and stretching and then a mean value for the composite obtained.

3. Results and Discussion

3.1. Species Identification

Placement of the samples in the COI tree suggested that coral colonies A, B and C were almost identical, while sample D differed from the others. Combined with information from the ITS phylogeny, the species identification revealed that coral colonies A, B and C belong to the species *Porites lobata* and coral D was identified as *Porites lichen*. *Porites lobata* is a common, cosmopolitan species. Both species co-occur in the tropical parts of the Indian Ocean (e.g., Cacciapaglia & van Woesik, 2018; Séré et al., 2012) and in the Pacific Ocean (e.g., D'Croz et al., 2001; Tisthammer & Richmond, 2018).

3.2. Metal Concentrations in Aquarium Water

The concentration of all metals used in this study was overall lower in the control system than in the metal system (Figure 3, Table S1). The concentrations of Cu and Sn were similar and high compared to the targeted values in both systems (Table 1), and no clear elevation was obtained in course of the subsequent culturing phases in the metal system. In the first phases 0 and 1, and also for Cr, Mn and Ag in Phase 2, the metal concentration in the control system was nearly the same as in the metal system. However, in phases 2, 3, and 4, the metal system showed elevated concentrations approaching target values for most metals. Distinct metal concentrations between culturing phases in the metal system were obtained for Ni, Zn, Ag, Cd, Hg, and Pb, and also Mn, even though the elevation between phases was less pronounced. At the beginning of each phase, most metal concentrations (Mn, Ni, Cu, Zn, Ag, Cd, Hg, and Pb) peaked and then declined again after 1 week. This feature was due to the addition of stock solution to reach the next concentration level and subsequent removal from the dissolved form.

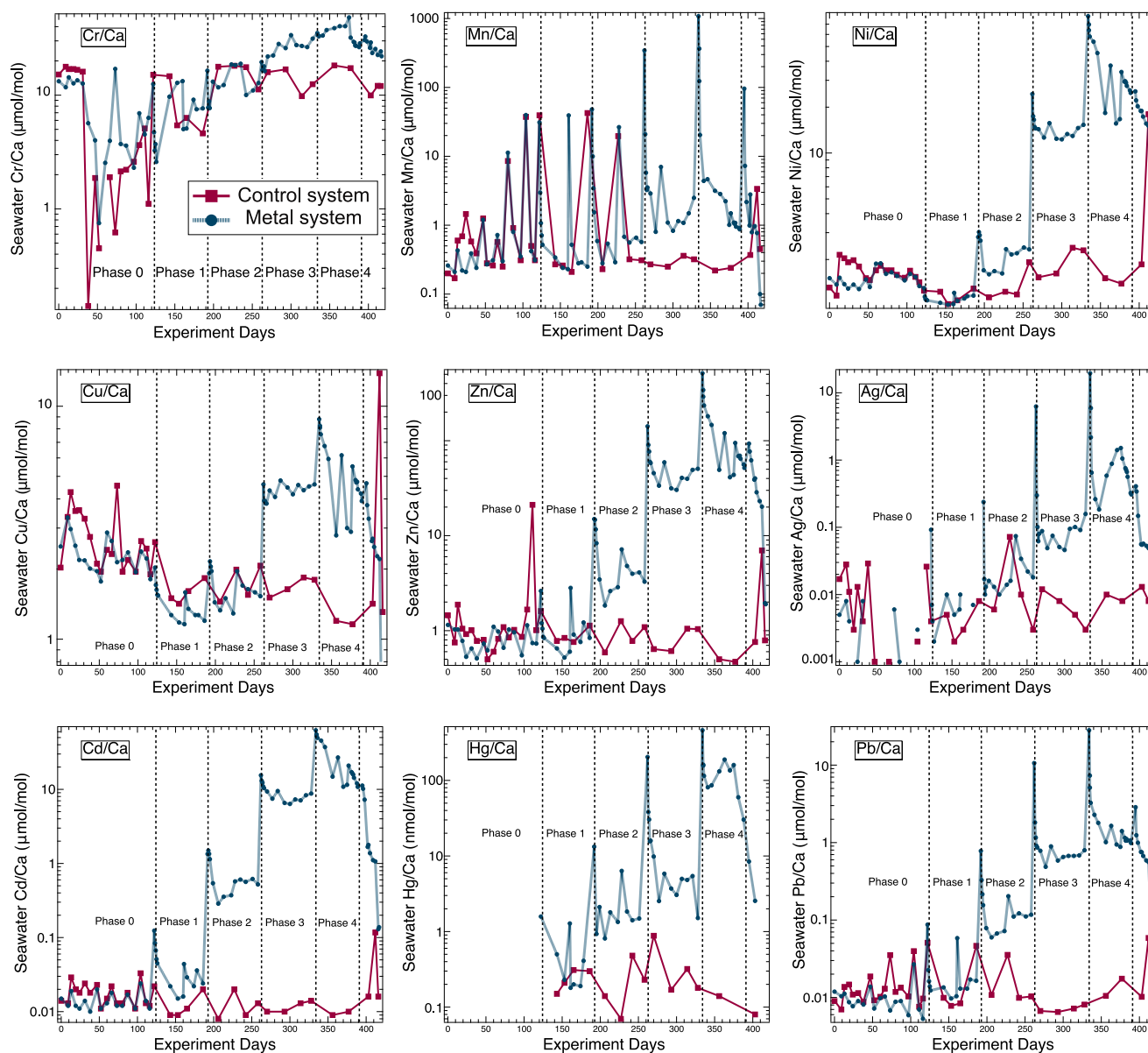


Figure 3. TE/Ca values ($\mu\text{mol/mol}$) in the culturing medium during phases 0 through four on a logarithmic scale. Note that the Hg/Ca values from Phase 0 of both systems are not given because no Hg samples were taken during this period.

Furthermore, smaller peaks within one culturing phase were linked to water exchange, when stock solution was added to balance the dilution of metals due to the addition of fresh seawater. The concentration in the control system was comparatively stable over the entire culturing period (Figure 3). A high scatter was found for Cr and Mn with sudden peaks in concentration. For Sn, the changes in the culturing seawater were very limited (Figure S1 in Supporting Information S1). After 10 weeks of Phase 4 the stock solution was exhausted and without further additions the trace metal concentration in the metal system decreased toward the end of the experiments. Excluding this drop at the end of the experiment, we compared the target metal concentrations with those measured for each phase (average across each treatment phase) to determine the experimental trueness for each metal (Actual/Target concentrations; Table 1). This was calculated by subtracting the mean concentration of Phase 0 to account for the starting background concentration in the system. This background compared well with the metal concentrations in the control tank but was higher in Phase 0 than Phase 1 for a few metals resulting in negative actual/target concentration ratios. Excluding these anomalous early phases, the trueness values range from 0.2 to 3.3 with many values consistently below 1 reflecting the constant removal of metals from the system.

These effects meant the experimental control was variable across the metals and can be classified into four categories; (a) systematic control over at least three phases (Zn, Cd, Hg, Pb), (b) control in most phases with high background spikes or variability also observed in the control tank (Mn, Ni), (c) only control in one or two phases because of high background levels (Cr, Cu, Ag), and (d) no control because of high background levels also observed in the control tank (Sn). The high background for some metals is likely the unavoidable consequence of the metal content of the salts used to maintain the required salinity. The lack of any control for Sn and decreasing concentrations through Phase 0 suggests some removal from the system.

The loss of metals could have occurred via several different processes. One possibility was the uptake by the accompanying organisms living in the culturing system, including algae growth. The protein skimmer, which ensured the oxygenation and skimmed proteins or exopolymers from the system, could also have removed metals adsorbed on these substances. Indeed, metal ions are surface reactive and it is therefore probable that some adhered to inner surface areas of system components, which included glass panes, tubing, hoses and the fiber filter for larger particles. As the surface space for adsorption was limited, it appears plausible that the concentration of metals was decreasing until all adsorption spaces were taken. Afterward, the concentration would be expected to stabilize and this was observed approximately 5 days after the input of the stock solution for Ni, Zn, Ag, Cd, Hg, and Pb (Figure 3). Having foreseen this possibility, we attempted to counteract adsorptive loss of metals by a regular addition of a certain amount of the stock solution to the metal system which worked better for some metals than others. The average per phase actual/target concentration ratios range from 0.2 to 3.3 (excluding the early phases and Sn) suggesting some removal of metals by the system. The peaks and declines of concentrations at the start of each phase also indicate the removal of metals from the system (Table 1). Phase 3 had actual/target concentration ratios above 1 for Ni, Zn, and Cd, and most of the actual/target concentration ratios suggest moderate removal producing a good control of seawater metal concentrations. Nevertheless, the short-term concentration changes were sometimes mirrored in the aragonite of the corals with spikes in concentration around steps between phases (Figure 2). This justified the inclusion of the high concentrations at the beginning of a phase for the calculation of average values for each phase and these peaks provide time markers for the coral skeleton data.

The loss of Hg from solution may have resulted from Hg being present in the water as methylmercury which the corals could not uptake but it is unlikely most of the Hg was present in this form given the light conditions (Jeremiason et al., 2015). Actual/target concentration ratios for total Hg were very consistent around 0.3 suggesting consistent loss from the system, perhaps as volatile Hg⁰. However, other metals which are not volatile like Pb exhibited similar actual/target concentration ratios (Table 1), suggesting a similar removal mechanism like adsorption to particles in the skimmer. It should also be noted that higher concentrations of metals, including Mn, Ni, Cu, Zn, Cd, and Pb, have been found in coral tissue, zooxanthellae and gametes compared to the skeleton (e.g., Reichelt-Brushett & McOrist, 2003), suggesting that the coral tissue and zooxanthellae may have removed some of the metals from solution. Coral tissues have not been analyzed in this study as it is ultimately the skeleton that is available to reconstruct past seawater metal concentrations across annual density bands.

3.3. Coral Skeleton Growth

Growth rates of the corals varied between sub-colonies and within an individual coral specimen but were comparable to those measured in field specimens (Table S2). Furthermore, we identified variations in the growth rate during different culturing phases and between the metal and the control system. It should be noted that coral D died 2.5 weeks after the exposure to the highest metal concentration in Phase 4. Overall, growth rates in this study did not show any clear trends as a response to the pollution metal concentrations.

3.4. Metal Incorporation Into Coral Skeleton

Although the samples were chemically cleaned to remove tissue and then pre-ablated with the laser, it cannot be determined through laser ablation ICP-MS analyses where the metals reside in the coral skeleton. The pre-ablation laser pass employs a large spot moving faster than typical analyses to remove any surface coatings or contamination. During the analyses the laser vaporises the skeletal aragonite and any inclusions to a depth of a few microns as it passes over. The *Porites* species used here have a relatively small polyp size and therefore a simple structure unlike many other corals, which is partly why they are the species of choice for paleo-climate studies using geochemical proxies. The laser spot would have averaged many structural units at once and replicated lines

parallel to each other to give a more representative result for each sample. The metals measured could be incorporated into the aragonite lattice, trapped in interstitial positions, or bound to an associated phase such as skeletal organic matter. This is in contrast to studies where the aragonite bound elements are isolated by repeated chemical treatments until no change in metal/Ca is observed (e.g., Shen & Boyle, 1988). Detectable (>3 times the limit of detection ($\text{LOD} = 3.3 \times \text{SD}$ of blank measurements)) amounts of all metals investigated were found in the skeleton of all four coral colonies, but the degree of incorporation varied greatly (Figures 4–6, Table 3). Differences between culturing phases occurred, and in some lines not all elements were detectable. The heavy metal concentration in the coral skeletons partly followed the concentration changes in the culturing medium with the exception of Sn and Hg (Figures 4–6 and Figures S2–S5 in Supporting Information S1 for all line measurements). For Sn, the changes in the culturing seawater were very limited (Figure S1 in Supporting Information S1) and therefore changes in the skeletal content are not expected. The Hg concentration in the coral skeleton of all colonies in all phases did not follow the concentration changes in the culturing medium.

Little increase in the skeletal metal concentrations was observed in phases 1 and 2, while most metals were elevated in the skeleton formed during phases 3 and 4. For example, the elevated seawater Cr concentration was mirrored in the skeleton of coral A in Phase 4, but this was not observed for corals B and D. The elevated Mn concentration in the seawater was recorded by all colonies in Phase 4 and in corals A and D partly during Phases 2 and 3. During Phase 4 and partly in Phase 3, all coral colonies had higher concentrations of Ni, Zn, Ag and Pb in their skeletons. Increased Cu concentrations in the coral skeleton were found in coral colonies A and B in Phase 4.

Although the concentration of total Hg in the experimental aquarium was increased stepwise (Table 2), the Hg/Ca in the coral skeleton remained low but variable between coral colonies subjected to the same treatment (Table 3). The lowest values are similar to those reported in previous studies following extensive cleaning to isolate aragonite bound Hg (Lamborg et al., 2013; R. Sun et al., 2016). With only the MACS powder pellet containing Hg in measurable quantities, which was used for the calibration, it was not possible to independently assess the quality of the Hg/Ca data like for the other metals. Even so, relatively consistent signals for the Hg/Ca of the MACS and the orders of magnitude changes in seawater Hg/Ca suggest a complex incorporation mechanism for Hg in coral skeletons.

3.4.1. Inter and Intra Colony Variability

Comparison between different colonies revealed no clear trends between colonies of the same species or between species. Generally, visual inspections revealed that polyps were extended and with good color suggesting all coral colonies were in good health over most of the culturing period. A loss of vitality was therefore not recognized as a biasing factor for the heavy metal incorporation into the coral skeleton. One clear exception was coral D, which died after 2.5 weeks in the highest metal Phase 4 and exhibited elevated TE/Ca values in the skeleton prior to death. Coral D belonged to the species *Porites lichen*, while the other three surviving colonies were *Porites lobata*, suggesting that mortality could be related to species.

Coral A displayed generally higher TE/Ca values than all other colonies for Cr, Mn, and Ni. Coral D (*P. lichen*) had higher concentrations of Ag and Pb in the skeleton compared to the other corals, which are all *Porites lobata*. Coral colony B had the lowest TE/Ca values for Cr, Mn, Zn, Ag, and Pb.

On coral colony A and C grown in the metal system, three lines were measured and clear differences between line A3 and C1, and the other lines were visible (Figures S2–S5 in Supporting Information S1). TE/Ca values were remarkably higher for Cr, Ni, Zn, Ag, Cd, and Pb compared to the other lines, which showed similar TE/Ca values. Four lines were measured on coral colony B of the metal system and all showed the same overall trends for all elements used in this study (Figure S3 in Supporting Information S1).

Part of the variability observed in the metal system was also found in the control system where the seawater metal content was relatively stable. Across the coral skeleton grown during the experiment, variability may be partly related to short term variations in the metal content of the seawater but is generally too high frequency (Figure 7), suggesting biomineralization effects. It is also clear from the observed intra and inter colony variability that biological processes most likely influence the metal uptake of corals. Essential elements like Mn, Ni or Zn could be consumed by the coral or symbiont cells, therefore reducing the metals available for incorporation into each coral skeleton. Non-essential elements like Cr, Cd, and Pb on the other hand could have been actively pumped out of the cell to prevent toxic and lethal effects, which could also attenuate metal incorporation.

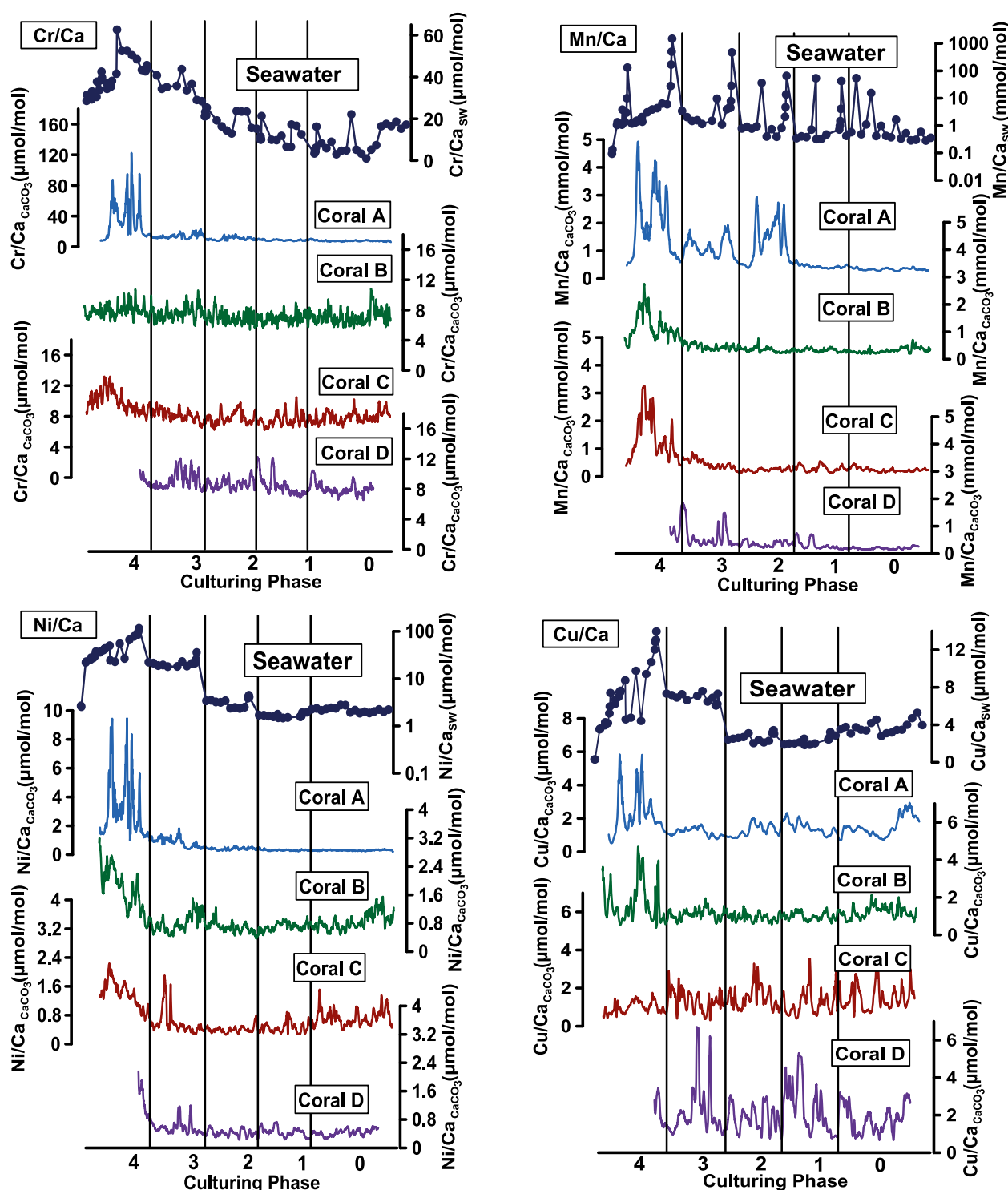


Figure 4. Composite line along the maximum growth axis profiles of Cr, Mn, Ni and Cu/Ca values of corals A, B, C, and D in the metal system measured by laser ablation ICP-MS (lower graphs) and corresponding TE/Ca values in the culturing seawater medium (upper graph). To facilitate a comparison, all coral and water lines were transformed to the same Y-scale and therefore, differences in growth rates cannot be seen in this figure (see Table S2 for growth rates). The lines represent a running average over five points. The composite line of all laser scans along the maximum growth axis per colony was calculated using QAnalyserie (Kotov & Päläike, 2018). Note that coral D died at the beginning of Phase 4 after approximately 2.5 weeks. Some elements are displayed with a logarithmic scale for the water measurements. All values can be found in Tables S1 and S2 and at PANGAEA (Schmidt, 2024, <https://doi.pangaea.de/10.1594/PANGAEA.938748>).

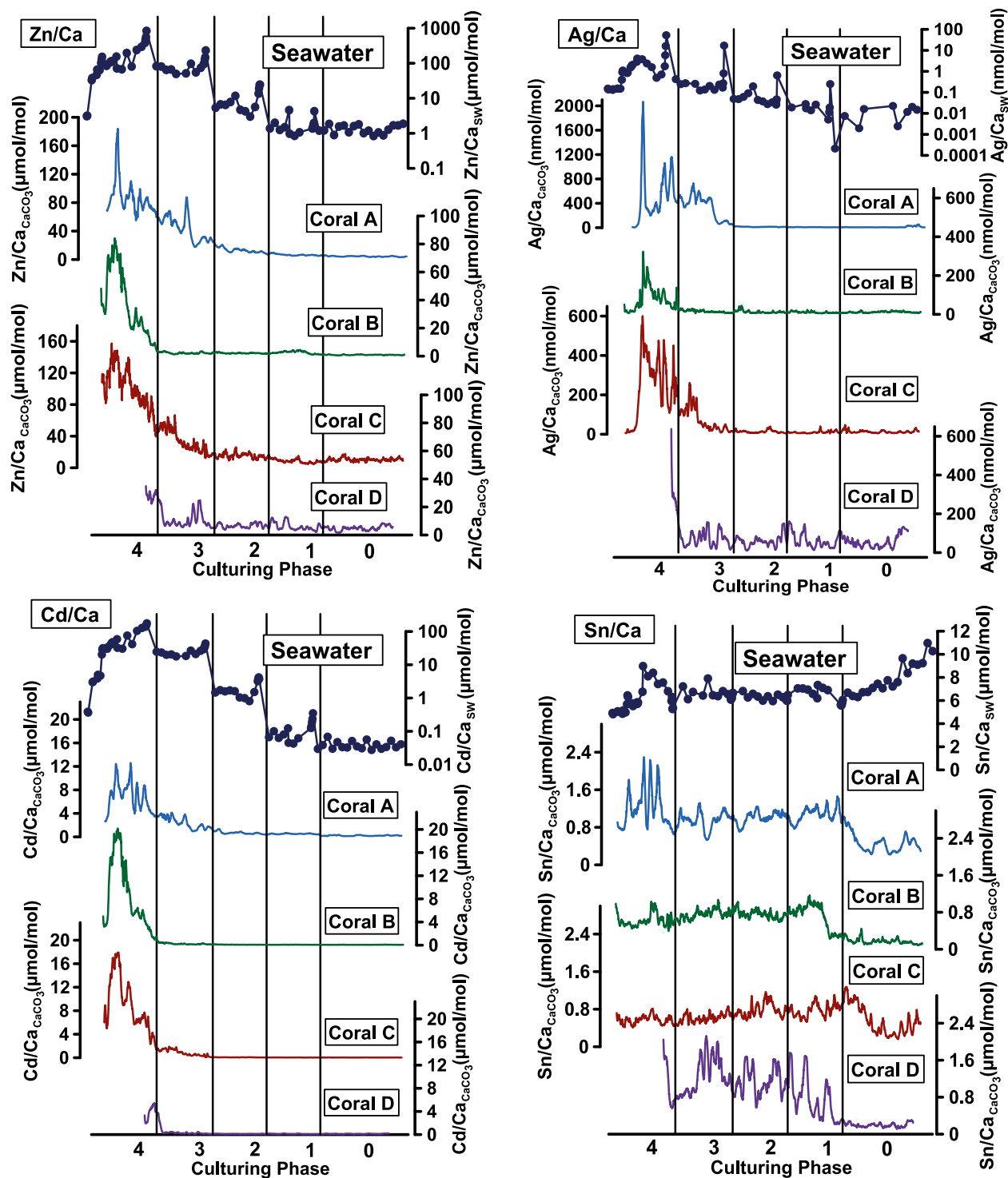


Figure 5. Composite line along the maximum growth axis profiles of Zn, Ag, Cd and Sn/Ca values of corals A, B, C and D in the metal system measured by laser ablation ICP-MS (lower graphs) and corresponding TE/Ca values in the culturing seawater medium (upper graph). To facilitate a comparison, all coral and water lines were transformed to the same Y-scale and therefore, differences in growth rates cannot be seen in this figure (see Table S2 for growth rates). The lines represent a running average over five points. The composite line of all laser scans along the maximum growth axis per colony was calculated using QAnalyserie (Kotov & Pälke, 2018). Note that coral D died at the beginning of Phase 4 after approximately 2.5 weeks. Some elements are displayed with a logarithmic scale for the water measurements. All values can be found in Tables S1 and S2 and at PANGAEA (Schmidt, 2024, <https://doi.pangaea.de/10.1594/PANGAEA.938748>).

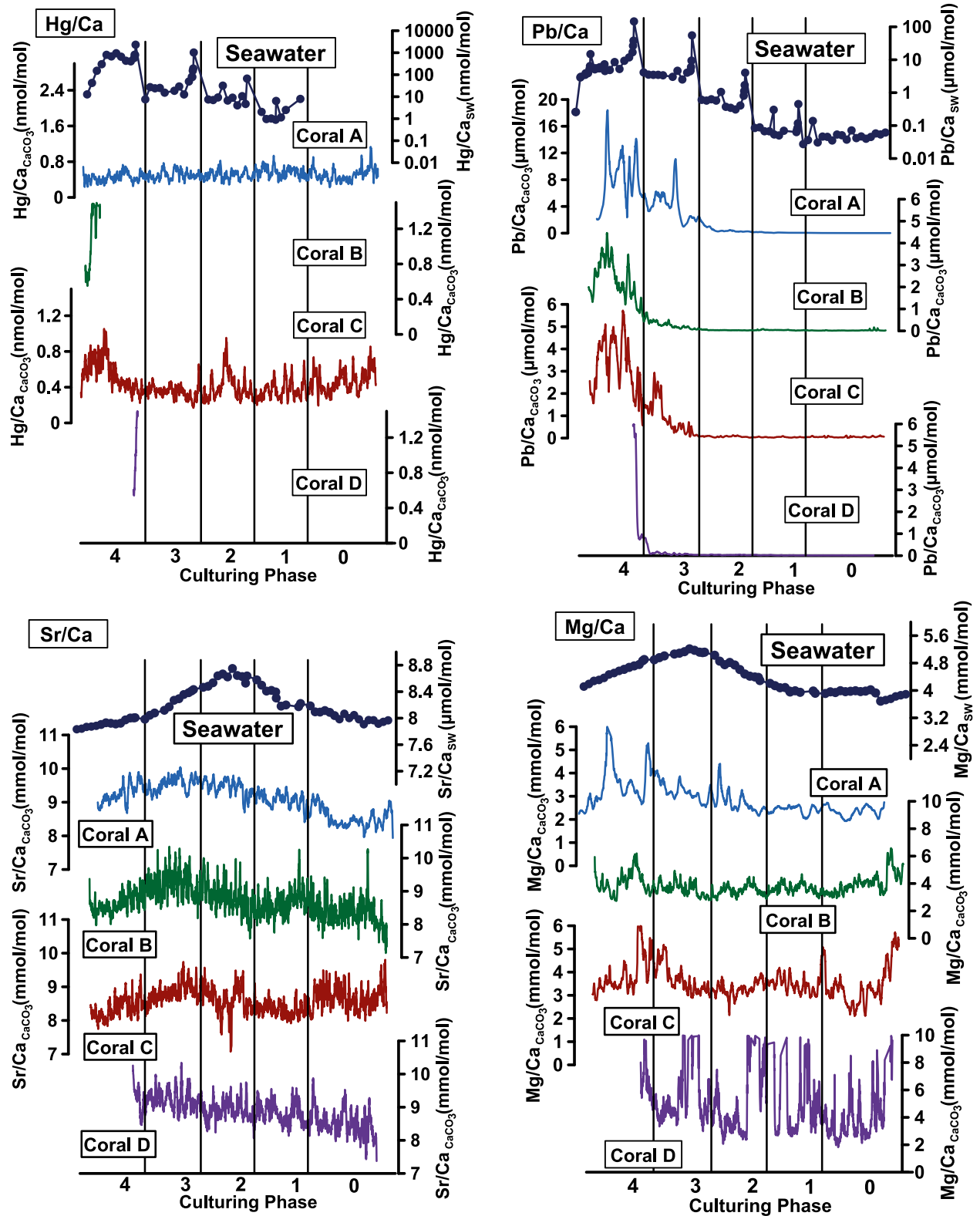


Figure 6.

3.5. Incorporation Mechanisms

Corals precipitate aragonite with the help of their extracellular calcicoblastic epithelium. This tissue contains calcifying cells that control the composition of the extracellular calcifying medium (ECM) located between the calcicoblastic ectoderm and pre-existing skeleton (e.g., Allemand et al., 2004, 2011; Tambutté et al., 2011). Different mechanisms are hypothesized to be involved in the transport of ions relevant for calcification from the seawater to this area. One mechanism is the transcellular calcium transport, that is, the transport of calcium ions through the cell membrane of the calcicoblastic epithelium via specific biomolecules building ion channels or ion exchangers (Allemand et al., 2004; Capasso et al., 2021). However, many cations other than Ca are also present in the ECM and subsequently in the coral skeleton, which led to the assumption that Ca transporters may also transport other ions similar to Ca in size and charge (e.g., Mn, Cd and perhaps Pb). Another route is direct seawater transport via paracellular pathways or via vacuoles (Gagnon et al., 2012; Mass et al., 2017; C.-Y. Sun et al., 2020). Erez and Braun (2007) found evidence for paracellular pathways by adding the fluorescent dyes Calcein and FITC-Dextran to seawater, which are too large to enter the skeleton through the transcellular route. This means that the composition of the coral skeleton is directly related to seawater chemistry, which enables corals to monitor seawater composition but at the same time allows metal speciation to influence incorporation.

Adsorption onto the skeletal surface was found in earlier studies to play a role during times of tissue retraction during stress (Amiel et al., 1973; Brown et al., 1991; St John, 1974). In our experiments no tissue retraction was observed. In coral D, which died suddenly, elevated heavy metal concentrations in the skeleton formed shortly before death. It is possible that adsorption of metals occurred not only on the surface but also across a zone of the exposed porous skeleton, otherwise adsorption is unlikely to have contributed to the metal concentration in the coral skeleton. Our cleaning procedure should additionally guarantee that as much contamination on the coral surface as possible was removed prior to analysis.

Metals can bind to organic matter in the coral lattice, which was indicated in previous studies (e.g., Allison & Finch, 2004; Bilings & Ragland, 1968; Shen et al., 1991). Most studies of both coral tissue and skeletal metal content find higher metal concentrations in the tissues (e.g., Reichelt-Brushett & McOrist, 2003). Cuif et al. (1999) showed that coral fasciculi consist of aragonite crystal bundles that are formed from repeated superimposition of micron thick growth layers. Organic compounds and metals such as Mg are concentrated at these boundaries (Cuif et al., 2003). Organic matter represents 1 to 2.5 wt% of the coral skeleton (Cuif et al., 2004) and it was found that trace elements concentrate with organic matter (Allison & Finch, 2004; Finch & Allison, 2008). It is possible that this mechanism contributed to the TE/Ca values of this study, with the laser analyzing all phases present. Mg profiles of the composite lines revealed elevated values during Phase 4 in the corals A to C, which could hint toward elevated organic matter content, and in turn elevated metals associated with this organic matter.

Besides Ca^{2+} substitution in the aragonite lattice and binding with skeletal organic matter, metals could also be located in interstitial positions and defects in the lattice. Such incorporation mechanisms could also result in correlations between the skeleton and seawater metal concentrations but would also be influenced by precipitation rate effects. A combination of different incorporation mechanisms could explain the non-linear incorporation found here. However, to investigate these possibilities would require synchrotron techniques (e.g., Finch & Allison, 2008) and most of the metals investigated here are likely present at too low concentrations for such analyses. Given these constraints, metals with an empirical calibration between seawater and aragonite concentrations can be used for the reconstruction of past seawater conditions, but more effort is needed to understand the complex and colony specific relationships observed.

Figure 6. Composite line along the maximum growth axis profiles of Hg, Pb, Sr, and Mg/Ca values of corals A, B, C, and D in the metal system measured by laser ablation ICP-MS (lower graphs) and corresponding TE/Ca values in the culturing seawater medium (upper graph). To facilitate a comparison, all coral and water lines were transformed to the same Y-scale and therefore, differences in growth rates cannot be seen in this figure (see Table S2 for growth rates). The lines represent a running average over five points. The composite line of all laser scans along the maximum growth axis per colony was calculated using QAnalyserie (Kotov & Pälke, 2018). Note that coral D died at the beginning of Phase 4 after approximately 2.5 weeks. Some elements are displayed with a logarithmic scale for the water measurements. All values can be found in Tables S1 and S2 and Table S4 in Supporting Information S1 and at PANGAEA (Schmidt, 2024, <https://doi.pangaea.de/10.1594/PANGAEA.938748>).

Table 3
Mean Metal/Ca Ratios, Standard Deviations, and Apparent Partition Coefficients (D_{TE}) of Composite Lines for Different Culturing Phases for All and Individual Colonies

Mean D_{TE}	Phase	Cr/Ca ($\mu\text{mol/mol}$)	Mn/Ca ($\mu\text{mol/mol}$)	Ni/Ca ($\mu\text{mol/mol}$)	Cu/Ca ($\mu\text{mol/mol}$)	Zn/Ca ($\mu\text{mol/mol}$)	Ag/Ca (nmol/mol)	Cd/Ca ($\mu\text{mol/mol}$)	Sn/Ca ($\mu\text{mol/mol}$)	Hg/Ca (nmol/mol)	Pb/Ca ($\mu\text{mol/mol}$)
Mean of all composites	0	0.98	0.084	0.37	0.63	5.84	4.96	7.46	0.13		2.53
Mean of all composites	1	1.05	0.056	0.43	1	5.56	1.38	3.6	0.39	18.17	1.71
Mean of all composites	2	0.66	0.076	0.22	0.87	1.46	0.65	0.32	0.44	2.29	0.59
Mean of all composites	3	0.4	0.026	0.05	0.31	0.44	0.34	0.17	0.36	0.15	1.11
Mean of all composites	4	0.46	0.014	0.05	0.36	0.44	0.33	0.23	0.51	0.01	1.61
Control colony means		1.029	0.097	1.019	2.41	6.926	4.09	7.633	0.822	0.145	2.542
Mean D_{TE} of all		0.76	0.059	0.36	0.93	3.44	1.96	3.23	0.44	4.16	1.68
Mean SD of all		0.3	0.033	0.36	0.78	2.98	2.04	3.58	0.23	7.89	0.77
SD of all composites	0	0.05	0.021	0.16	0.08	4.24	4.52	5.49	0.08		1.75
SD of all composites	1	0.1	0.008	0.16	0.37	3.07	1.67	3.95	0.06	19.62	0.61
SD of all composites	2	0.11	0.06	0.06	0.27	0.91	0.65	0.31	0.11	2.5	0.52
SD of all composites	3	0.11	0.011	0.01	0.07	0.29	0.32	0.14	0.08	0.22	0.92
SD of all composites	4	0.35	0.004	0.02	0.15	0.23	0.43	0.08	0.32	0.02	1.04
Control SD		0.094	0.045	1.426	2.311	4.317	1.918	6.269	0.267	0.265	0.768
Coral A	Phase	Cr/Ca	Mn/Ca	Ni/Ca	Cu/Ca	Zn/Ca	Ag/Ca	Cd/Ca	Sn/Ca	Hg/Ca	Pb/Ca
Coral A, Composite Line	0	7.48	0.33	0.3	1.57	4.28	12.23	0.21	0.4	0.5	0.02
Coral A, Composite Line	1	8.37	0.4	0.3	1.32	5.5	7.14	0.42	1.02	0.56	0.05
Coral A, Composite Line	2	10.25	1.19	0.39	1.41	10.78	11.19	0.58	0.99	0.51	0.25
Coral A, Composite Line	3	13.16	1.07	0.78	1.16	38.52	252.31	2.17	0.95	0.5	3.49
Coral A, Composite Line	4	33.02	1.88	2.99	2.25	83.6	492.12	6.49	1.21	0.44	7.49
Standard Error											
Coral A, Composite Line	0	0.04	0.003	0.002	0.04	0.03	0.93	0	0.01	0.02	0.0003
Coral A, Composite Line	1	0.05	0.005	0.003	0.02	0.05	0.14	0.01	0.02	0.01	0.001
Coral A, Composite Line	2	0.14	0.05	0.01	0.02	0.15	0.29	0.01	0.01	0.01	0.01
Coral A, Composite Line	3	0.2	0.02	0.02	0.02	1.04	12.26	0.07	0.01	0.01	0.13
Coral A, Composite Line	4	1.43	0.09	0.13	0.1	1.72	27.64	0.18	0.03	0.01	0.25
D_{TE} Single Phases											
Coral A, Composite Line	0	0.96	0.1	0.2	0.67	5.16	2.7	14.91	0.15	0	2.02
Coral A, Composite Line	1	1.12	0.07	0.27	0.92	4.8	0.45	9.44	0.47	1.59	2.14
Coral A, Composite Line	2	0.8	0.17	0.17	0.83	1.67	0.29	0.77	0.47	0.21	1.34
Coral A, Composite Line	3	0.56	0.04	0.05	0.27	0.67	0.47	0.23	0.43	0.02	2.26
Coral A, Composite Line	4	0.98	0.02	0.08	0.41	0.58	0.22	0.23	0.55	0	2.11
Mean D_{TE}		0.88	0.08	0.15	0.62	2.58	0.83	5.12	0.41	0.46	1.98

Table 3
Continued

Coral A	Phase	Cr/Ca	Mn/Ca	Ni/Ca	Cu/Ca	Zn/Ca	Ag/Ca	Cd/Ca	Sn/Ca	Hg/Ca	Pb/Ca
±SD		0.22	0.06	0.09	0.27	2.24	1.05	6.73	0.15	0.76	0.36
Slope D_{TE}		0.85	0.01	0.07	na	0.55	0.24	0.23	na	na	2.12
Correlation coefficient (R^2)		0.839	0.74	0.96		0.998	0.92976	0.997			0.998
Significance (p)		0.03	0.06	0.0033		0.000034	0.001	0.000023			0.000000359
Coral B	Phase	Cr/Ca	Mn/Ca	Ni/Ca	Cu/Ca	Zn/Ca	Ag/Ca	Cd/Ca	Sn/Ca	Hg/Ca	Pb/Ca
Coral B—Composite Line	0	7.1	0.32	0.85	1.2	0.9	11.56	0.07	0.18	12.24	0.02
Coral B—Composite Line	1	6.9	0.33	0.72	1	2.57	10.37	0.07	0.74	13.37	0.04
Coral B—Composite Line	2	7.06	0.34	0.67	0.96	2.1	12.67	0.08	0.76	12.31	0.03
Coral B—Composite Line	3	7.6	0.45	0.81	1.09	2.22	14.44	0.21	0.76	11.74	0.24
Coral B—Composite Line	4	7.94	1.13	1.61	1.71	34.92	75.43	7.62	0.63	4.57	2.16
Standard Error											
Coral B—Composite Line	0	0.04	0.003	0.01	0.01	0.01	0.13	0.0005	0.002	0.14	0.001
Coral B—Composite Line	1	0.04	0.003	0.005	0.01	0.04	0.18	0.001	0.01	0.12	0.001
Coral B—Composite Line	2	0.04	0.004	0.01	0.01	0.01	0.32	0.001	0.004	0.11	0.0005
Coral B—Composite Line	3	0.04	0.004	0.01	0.01	0.02	0.25	0.003	0.005	0.12	0.01
Coral B—Composite Line	4	0.04	0.02	0.02	0.04	0.85	2.26	0.22	0.01	0.1	0.03
D_{TE} Single Phases											
D_{TE} Single Phases	0	0.92	0.1	0.565	0.51	1.09	2.55	4.97	0.07	0	2.02
D_{TE} Single Phases	1	0.92	0.055	0.647	0.69	2.24	0.65	1.57	0.34	37.99	1.71
D_{TE} Single Phases	2	0.55	0.047	0.296	0.57	0.33	0.33	0.11	0.36	5.1	0.16
D_{TE} Single Phases	3	0.32	0.016	0.054	0.25	0.04	0.03	0.02	0.34	0.47	0.16
D_{TE} Single Phases	4	0.24	0.012	0.042	0.31	0.24	0.03	0.27	0.29	0.04	0.61
Mean D_{TE}	0	0.59	0.046	0.321	0.47	0.79	0.72	1.39	0.28	10.9	0.93
±SD	0	0.32	0.036	0.281	0.18	0.9	1.06	2.1	0.12	18.2	0.88
Slope D_{TE}	0	0.037	0.0089	0.0224	na	0.221	0.034	0.247	na	na	0.5355
Correlation coefficient (R^2)	0	0.9795	0.988	0.88	na	0.856	0.96	0.899	na	na	0.8919
Significance (p)	0	0.004	0.0006	0.017	na	0.024	0.00118	0.0025	na	na	0.0025
Coral C	Phase	Cr/Ca	Mn/Ca	Ni/Ca	Cu/Ca	Zn/Ca	Ag/Ca	Cd/Ca	Sn/Ca	Hg/Ca	Pb/Ca
Coral C—Composite Line	0	7.85	0.24	0.67	1.44	9.45	12.89	0.03	0.62	0.44	0.05
Coral C—Composite Line	1	7.57	0.29	0.46	1.22	11.05	8.57	0.04	0.76	0.36	0.05
Coral C—Composite Line	2	7.66	0.23	0.39	1.46	16.29	14.16	0.09	0.75	0.37	0.09
Coral C—Composite Line	3	8.37	0.49	0.61	1.28	35.5	75.9	0.86	0.59	0.36	0.98
Coral C—Composite Line	4	10.05	1.26	1.29	0.98	99.04	231.79	8.25	0.57	0.57	3.16
Standard Error											
Coral C—Composite Line	0	0.03	0.002	0.01	0.02	0.06	0.22	0.0003	0.01	0.01	0.001
Coral C—Composite Line	1	0.04	0.004	0.01	0.02	0.1	0.15	0.0005	0.01	0.01	0.001
Coral C—Composite Line	2	0.03	0.003	0.003	0.02	0.13	0.33	0.004	0.01	0.01	0.002
Coral C—Composite Line	3	0.03	0.01	0.01	0.02	0.49	2.28	0.02	0.004	0.01	0.03
Coral C—Composite Line	4	0.05	0.03	0.01	0.01	0.93	5.32	0.16	0.004	0.01	0.04
D_{TE} Single Phases											
D_{TE} Single Phases	0	1.01	0.075	0.446	0.62	11.4	2.84	2.13	0.23	0	5.06
D_{TE} Single Phases	1	1.01	0.048	0.414	0.85	9.64	0.54	0.9	0.35	1.02	2.14

Table 3
Continued

Coral C	Phase	Cr/Ca	Mn/Ca	Ni/Ca	Cu/Ca	Zn/Ca	Ag/Ca	Cd/Ca	Sn/Ca	Hg/Ca	Pb/Ca
D _{TE} Single Phases	2	0.59	0.032	0.172	0.86	2.53	0.37	0.12	0.35	0.15	0.48
D _{TE} Single Phases	3	0.35	0.017	0.04	0.3	0.62	0.14	0.09	0.26	0.01	0.63
D _{TE} Single Phases	4	0.3	0.013	0.033	0.18	0.69	0.1	0.3	0.26	0.01	0.89
Mean D _{TE}		0.65	0.037	0.221	0.56	4.97	0.8	0.71	0.29	0.3	1.84
±SD		0.35	0.025	0.199	0.31	5.16	1.16	0.86	0.06	0.49	1.91
Slope D _{TE}		0.084	0.011	0.02	na	0.606	0.107	0.274	na	na	0.849
Correlation coefficient (<i>R</i> ²)		0.869	0.996	0.859	na	0.98	0.997	0.942	na	na	0.983
Significance (<i>p</i>)		0.026	0.000118	0.023	na	0.0009	0.00004	0.00085	na	na	0.000058
Coral D	Phase	Cr/Ca	Mn/Ca	Ni/Ca	Cu/Ca	Zn/Ca	Ag/Ca	Cd/Ca	Sn/Ca	Hg/Ca	Pb/Ca
Coral D—Composite Line (=Line 1)	0	7.84	0.19	0.42	1.64	4.72	53.17	0.11	0.21	6.74	0.01
Coral D—Composite Line (=Line 1)	1	8.61	0.32	0.43	2.21	6.36	62.04	0.11	0.92	11.29	0.02
Coral D—Composite Line (=Line 1)	2	8.93	0.44	0.51	2.06	8.41	61.98	0.21	1.25	8.95	0.07
Coral D—Composite Line (=Line 1)	3	8.84	0.94	1.03	1.76	24.44	397.15	3.09	0.95	2.37	2.14
Coral D—Composite Line (=Line 1)	4	10.52	0.99	2.26	2.84	35.51	2142.55	3.11	2.1	0.57	10.06
Standard Error											
Coral D—Composite Line (=Line 1)	0	0.03	0.002	0.004	0.02	0.05	0.97	0.001	0.002	0.06	0.0001
Coral D—Composite Line (=Line 1)	1	0.04	0	0.004	0.03	0.07	1.1	0.001	0.01	0.08	0.0003
Coral D—Composite Line (=Line 1)	2	0.05	0.01	0.006	0.04	0.13	1.21	0.004	0.01	0.09	0.0013
Coral D—Composite Line (=Line 1)	3	0.07	0.03	0.03	0.05	0.43	27.19	0.12	0.02	0.06	0.16
Coral D—Composite Line (=Line 1)	4	0.16	0.07	0.14	0.17	1.97	224.11	0.3	0.07	0.05	0.75
D _{TE} Single Phases											
D _{TE} Single Phases	0	1.01	0.059	0.279	0.7	5.69	11.73	7.81	0.08		1.01
D _{TE} Single Phases	1	1.15	0.053	0.387	1.53	5.55	3.87	2.47	0.42	32.08	0.86
D _{TE} Single Phases	2	0.69	0.061	0.225	1.21	1.3	1.62	0.28	0.59	3.71	0.38
D _{TE} Single Phases	3	0.37	0.033	0.068	0.41	0.42	0.74	0.33	0.43	0.1	1.39
D _{TE} Single Phases	4	0.31	0.01	0.058	0.52	0.25	0.97	0.11	0.95	0.01	2.83
Mean D _{TE}		0.71	0.044	0.204	0.88	2.64	3.79	2.2	0.49	8.97	1.29
±SD		0.37	0.022	0.141	0.48	2.75	4.61	3.28	0.32	15.5	0.93
Slope D _{TE}		0.0755	0.0076	0.0485	na	0.214	0.958	0.134	na	na	2.598
Correlation coefficient (<i>R</i> ²)		0.77	0.65	0.997	0	0.948	0.994	0.71	0	0	0.95
Significance (<i>p</i>)		0.049	0.0988	0.000055	0	0.005	0.00007	0.01	0	0	0.000599
Control lines	Cr/Ca	Mn/Ca	Ni/Ca	Cu/Ca	Zn/Ca	Ag/Ca	Cd/Ca	Sn/Ca	Hg/Ca	Pb/Ca	
CR2_L1	5	0.25	0.34	1.23	12.77	27.31	0.24	0.98	0.0905	0.03	
CR2_L2	17.15	0.26	0.82	27.85	25.81	121.27	0.38	3.92	0.1921	0.06	
BR_L1	10.22	0.36	1.08	4.53	3.19	35.01	0.05	1.46	0.0005	0.03	
BR_L2	7.95	0.19	0.51	1.25	2.82	13.96	0.03	1.02	0.0003	0.02	
AR_L1	7.24	0.21	1.09	1.34	8.01	12.44	0.06	1.14	0.0258	0.03	
AR_L2	7.9	0.53	1.01	1.94	9.24	31.59	0.05	1.18	0.0049	0.04	
AR_L3	20.33	1.12	19.92	14.79	35.02	84.15	0.28	3.2	0.0015	0.11	
AR_L4	8.89	0.45	4.84	3.41	8.46	23.06	0.03	1.56	0.002	0.04	
DR_L1	10.74	0.65	0.58	1.58	8.61	43.26	0.1	1.34	0.0012	0.04	

Table 3
Continued

Control lines	Cr/Ca	Mn/Ca	Ni/Ca	Cu/Ca	Zn/Ca	Ag/Ca	Cd/Ca	Sn/Ca	Hg/Ca	Pb/Ca
Control colony means										
Coral A mean	11.09	0.58	6.72	5.37	15.18	37.81	0.11	1.77	0.0085	0.06
Coral A SD	6.2	0.38	8.98	6.34	13.23	31.87	0.12	0.97	0.0116	0.03
Coral B mean	9.08	0.27	0.79	2.89	3.01	24.49	0.04	1.24	0.0004	0.03
Coral B SD	1.6	0.12	0.41	2.32	0.26	14.88	0.02	0.31	0.0002	0.01
Coral C mean	11.07	0.26	0.58	14.54	19.29	74.29	0.31	2.45	0.14	0.04
Coral C SD	8.59	0	0.34	18.82	9.22	66.44	0.1	2.08	0.07	0.03
Mean all control	10.6	0.45	3.36	6.44	12.66	43.56	0.14	1.76	0.04	0.04
SD all control	4.97	0.3	6.36	9.12	10.76	36.11	0.13	1.06	0.07	0.03
Control D_{TE}										
DR_L1	1.053	0.144	0.274	0.625	5.175	3.935	5.64	0.646	0.005	2.364
Coral A mean	1.087	0.127	3.156	2.124	9.126	3.439	5.864	0.856	0.033	3.463
Coral B mean	0.89	0.06	0.372	1.141	1.808	2.227	2.312	0.6	0.002	1.618
Coral C mean	1.085	0.057	0.273	5.748	11.596	6.757	16.715	1.187	0.541	2.724
Control Mean	1.029	0.097	1.019	2.41	6.926	4.09	7.633	0.822	0.145	2.542
SD	0.094	0.045	1.426	2.311	4.317	1.918	6.269	0.267	0.265	0.768

3.6. Partition Coefficient D_{TE}

Partition coefficients for the different trace elements were calculated from the molar coral skeleton TE/Ca and the average values of the aquarium water from the corresponding culturing phase (sampling was similarly spaced between phases so no weighting was applied). Composite line data were used to provide the most representative values for each colony (Table 3). Ideally D_{TE} values represent the regression line slope of a positive correlation between seawater TE/Ca and coral aragonite TE/Ca ($p < 0.05$, $R^2 \geq 0.45$). Such a correlation suggests a linear response of the coral skeleton concentration to changes in seawater concentration, a prerequisite for any quantitative reconstruction of past seawater chemistry. However, although statistically significant correlations were found for most metals (Figure 8, Table 3), it is clear from the regression plots that the incorporation for many

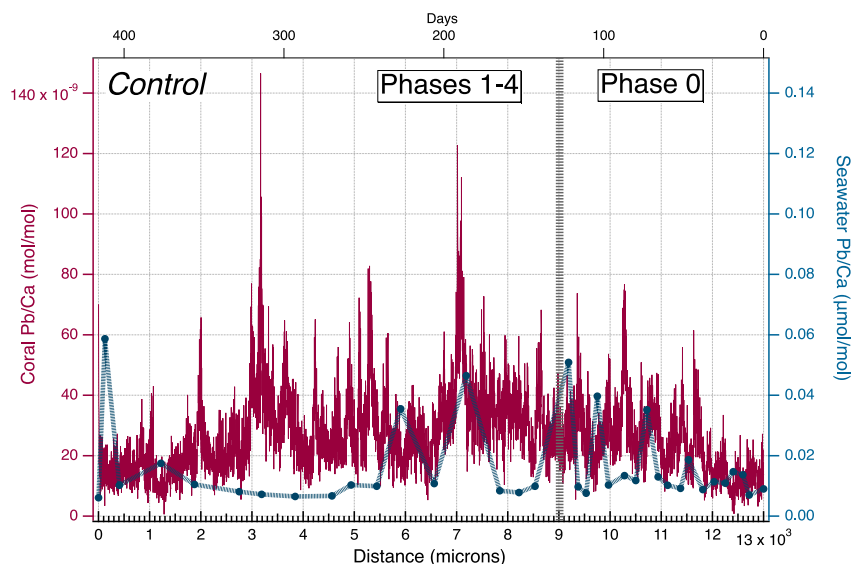


Figure 7. Example of variability of Pb/Ca ratios in the control system seawater and the resulting variability across the aragonite skeleton of one of the colonies which grew in the control system.

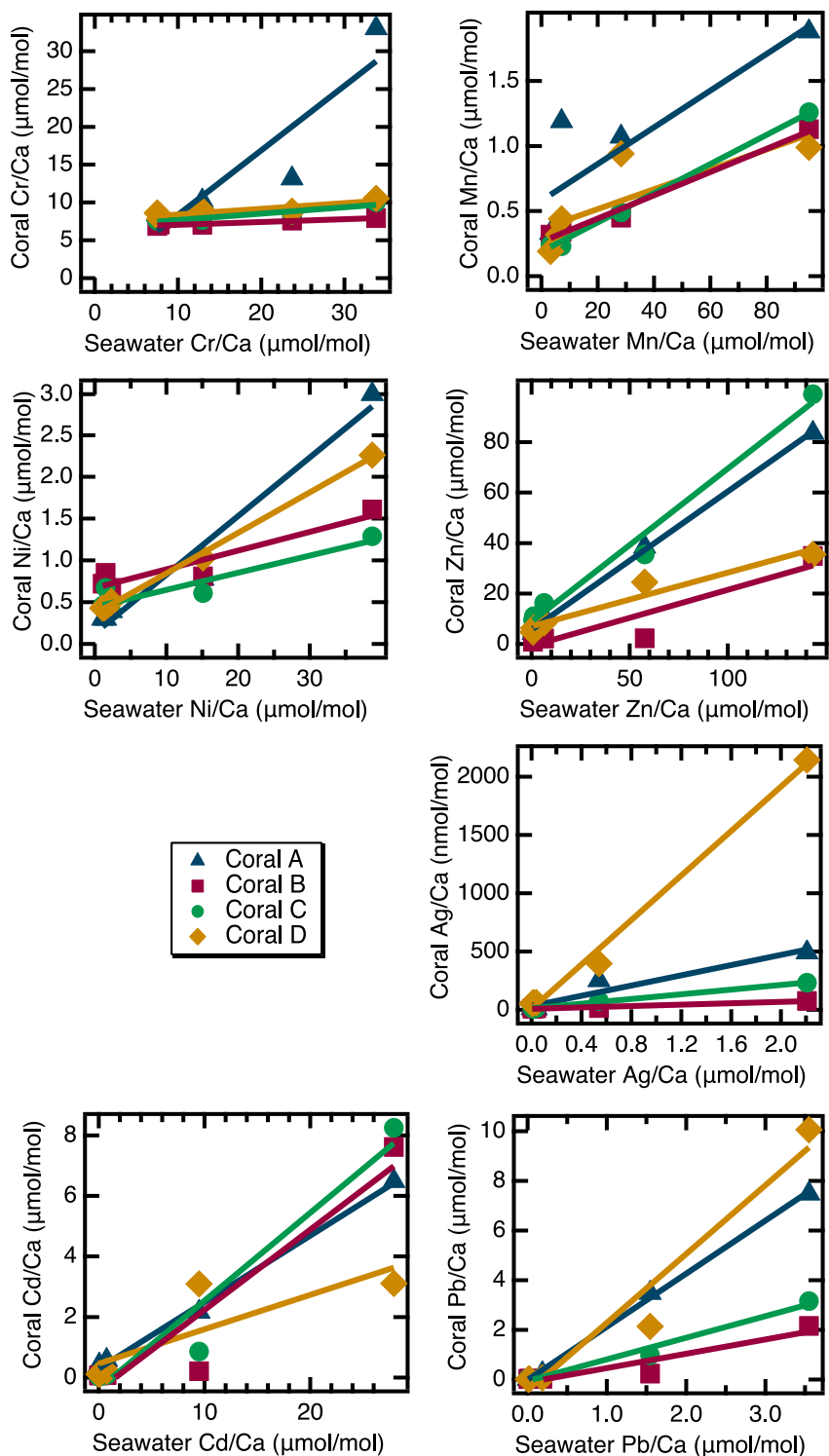


Figure 8. Regression of metal/Ca values of the composite line per colony in the metal system versus the TE/Ca values in the corresponding culturing medium based on Phases 0 to 4. Each data point represents the averaged phase value plotted against the mean metal concentrations in the seawater averaged over the culturing phase (Table 3). D_{TE} ($\pm SE$) values from the slope of the regression line and the regression statistics are given in Table 3. For Pb/Ca, the regressions could be forced through the origin.

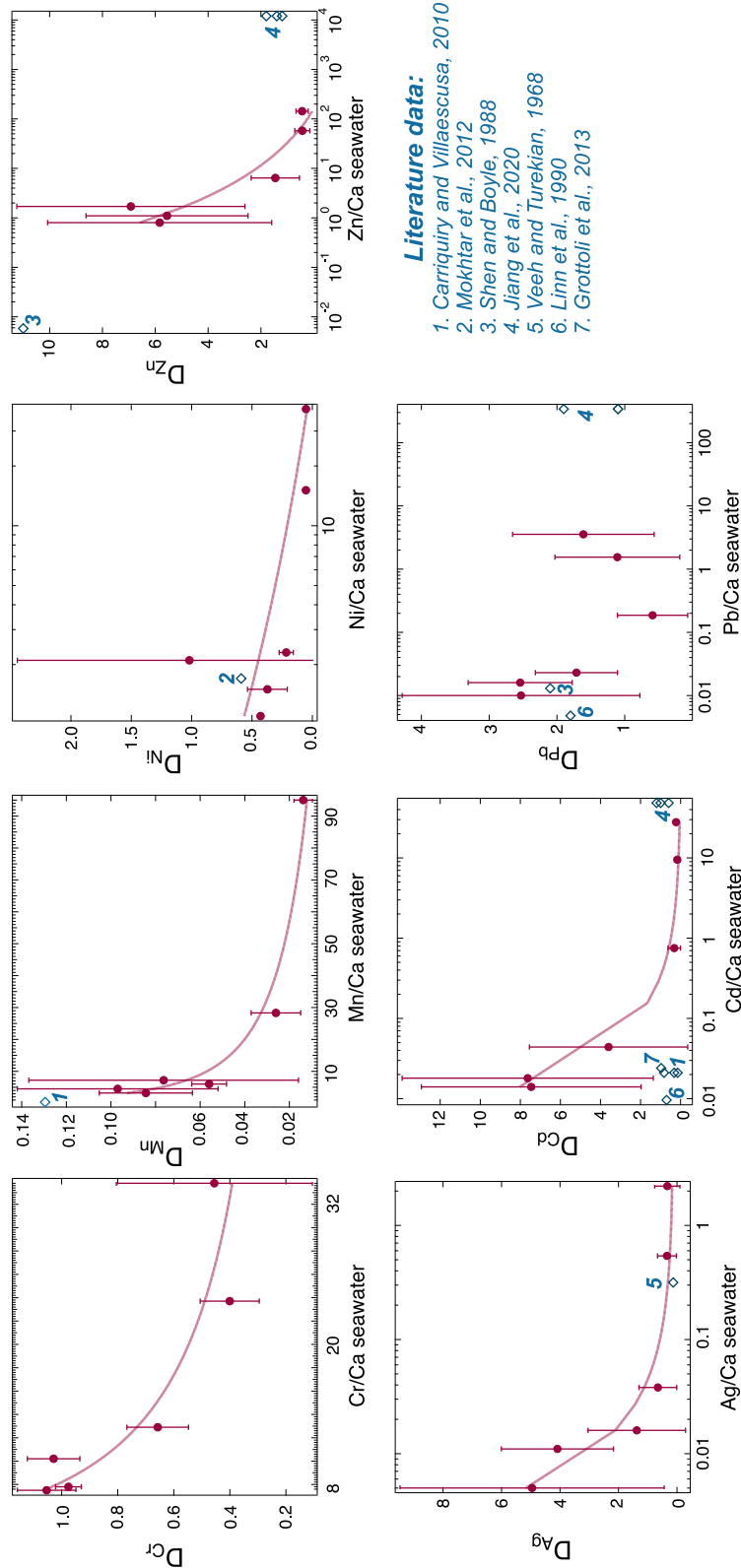


Figure 9. Comparison of D_{TE} values of this study with D_{TE} values from literature of different coral species (Table S3). The mean from the composite lines from each experimental phase and control D_{TE} and the SD from the different coral colonies are plotted as error bars (Table 3). D_{TE} values are based on the correlation between TE/Ca in seawater and the coral skeleton.

metals appears to be non-linear (Figure 9). The notable exception is Pb, for which it was even possible to force the intercept through the origin, indicating a robust linear response of coral Pb/Ca to changes in seawater Pb/Ca.

All D_{TE} values were also calculated separately for the average of every individual phase (Table 3). These average D_{TE} values are more akin to those existing in the literature where the average of 5 years of coral growth (Prouty et al., 2008 in Saha et al., 2016) or approximately 1 year of growth of small samples (Jiang et al., 2020) have been measured and compared to estimated seawater values for the growth period. The D_{TE} values derived this way tend to decrease with increasing seawater metal/Ca toward the values obtained by linear regression (Table 3). This indicates that the significant linear correlations are strongly controlled by the final culturing phase with the highest metal/Ca ratios. This hints toward an overload effect, which was also described for other organisms, for example, foraminifera (Munsel et al., 2010; Nardelli et al., 2016). It was suggested, that this effect comes into action as soon as the metal concentration exceeds a threshold above which intoxication is imminent and then biochemical mechanisms expelling metals or blocking the metal uptake occur. Alternatively, higher metal concentrations could influence partitioning through inhibitory effects reducing calcification rates, analogous to that observed for rare earth metals and calcite (Zhong & Mucci, 1995).

The non-linear response of the partitioning of many of the metals is revealed by plotting the D_{TE} values against the seawater metal/Ca with a power law curve fit to the data (Figure 9). For comparison, D_{TE} values estimated by previous studies have been compiled (Table S3) and where possible added to these plots. This comparison suggests that some differences in reported DTE values in previous work could be the result of the non-linear response observed here. The comparison also highlights the enormous differences between the observed seawater metal/Ca of studies looking at natural geogenic variations and those of strongly polluted waters (e.g., Figure 9 Zn/Ca). Generally, the D_{TE} values estimated by previous studies fall within the range observed here (Figure 9, Table S3), suggesting that reconstruction of the heavy metal concentration in seawater for ecosystem monitoring is possible. Many earlier studies employed more intensive cleaning procedures involving oxidative and reductive chemical treatments prior to analysis (Table S3) but the generally good agreement with TE/Ca values observed here suggests, for such cultured corals at least, such extensive cleaning is not necessary. The non-linear response approximating a power law complicates using the content of these metals as a quantitative proxy for past seawater metal concentrations but suggests relative stability of partitioning at high seawater metal/Ca. However, the non-linear response approximating a power law requires confirmation under different experimental conditions and in the field. Additionally, the high variability within and between coral colonies requires further study and suggests that multiple records from multiple coral colonies should be combined to obtain robust reconstructions.

4. Conclusions

Culturing experiments exposed *Porites lobata* and *Porites lichen* to a mixture of 10 different metals (Cr, Mn, Ni, Cu, Zn, Ag, Cd, Sn, Hg, and Pb) at increasing concentrations. Inter-colony differences in TE/Ca values occurred, but did not follow any systematic patterns and could not be linked to different growth rates. Cr, Mn, Ni, Zn, Ag, Cd and Pb showed a positive linear relationship between the heavy metal concentration in the coral skeleton and the culturing medium suggesting that the uptake of these metals mainly depended on their concentration in seawater. Hg concentrations in the aquarium seawater were increased over a large range, but Hg/Ca values in the coral skeleton remained low. Relationships with Cu/Ca and Sn/Ca could also not be established due to a lack of control of the seawater concentrations during the coral growth. Empirical partition coefficients (D_{TE}) from the mean of the individual coral composite lines \pm the standard deviation are Cr/Ca = 0.76 ± 0.3 , Mn/Ca = 0.059 ± 0.033 , Ni/Ca = 0.36 ± 0.36 , Zn/Ca = 3.44 ± 2.98 , Ag/Ca = 1.96 ± 2.04 , Cd/Ca = 3.23 ± 3.58 , and Pb/Ca = 1.68 ± 0.77 . The range of the D_{TE} values generally overlaps those reported by previous studies. These new data provide insights into the uptake of heavy metals by corals and therefore facilitate the use of coral skeletons as a promising tool for reconstructing reef environment metal concentrations.

Conflict of Interest

The authors declare no conflicts of interest relevant to this study.

Data Availability Statement

All data generated or analyzed during this study are either included in this article or are available at PANGAEA (Schmidt, 2024).

Acknowledgments

We thank Anton Eisenhauer and Florian Böhm for the host aquarium and help with the experimental aquaria whenever needed. The association “Kieler Aquarienfreunde” gave important input on coral aquaria and helped in finding the coral colonies commercially. The company Whitecorals provided the culturing system and was always open for questions. Claas Hiebenthal, KIMOCC, helped with the system design and provided system parts as well as technical support. Marlene Wall provided advice and shared system parts. Clara Wichmann and Anja Conventz helped maintain the systems and conducted sampling. Regina Surberg carried out the ICP-OES measurements, Ana Kolevica maintained the ICP-MS and Ulrike Westernströer helped with the laser ablation measurements. Sven Marquardt helped with the data handling. This work was supported by GEOMAR Helmholtz Centre for Ocean Research Kiel. Open Access funding enabled and organized by Projekt DEAL.

References

Abdo, S. Y., Duliu, O. G., Zinicovscaia, I., Sherif, M. M., & Frontasyeva, M. V. (2017). Epithermal neutron activation analysis of major and trace elements in Red Sea scleractinian corals. *Journal of Radioanalytical and Nuclear Chemistry*, 314(2), 1445–1452. <https://doi.org/10.1007/s10967-017-5511-8>

Alibert, C., Kinsley, L., Fallon, S. J., McCulloch, M. T., Berkelmans, R., & McAllister, F. (2003). Source of trace element variability in Great Barrier Reef corals affected by the Burdekin flood plumes. *Geochimica et Cosmochimica Acta*, 67(2), 231–246. [https://doi.org/10.1016/S0016-7037\(02\)01055-4](https://doi.org/10.1016/S0016-7037(02)01055-4)

Alibert, C., & McCulloch, M. T. (1997). Strontium/calcium ratios in modern porites corals from the Great Barrier Reef as a proxy for sea surface temperature: Calibration of the thermometer and monitoring of ENSO. *Paleoceanography*, 12(3), 345–363. <https://doi.org/10.1029/97PA00318>

Allemand, D., Ferrier-Pagès, C., Furla, P., Houlbrèque, F., Puverel, S., Reynaud, S., et al. (2004). Biomineralisation in reef-building corals: From molecular mechanisms to environmental control. *Comptes Rendus Palevol*, 3(6–7), 453–467. <https://doi.org/10.1016/j.crpv.2004.07.011>

Allemand, D., Tambutté, É., Zoccola, D., & Tambutté, S. (2011). Coral calcification, cells to reefs. *Coral Reefs: An Ecosystem in Transition*, 119–150. https://doi.org/10.1007/978-94-007-0114-4_9

Allison, N., Cohen, I., Finch, A. A., Erez, J., & Tudhope, A. W. (2014). Corals concentrate dissolved inorganic carbon to facilitate calcification. *Nature Communications*, 5, 1–6. <https://doi.org/10.1038/ncomms6741>

Allison, N., & Finch, A. A. (2004). High-resolution Sr/Ca records in modern *Porites lobata* corals: Effects of skeletal extension rate and architecture. *Geochemistry, Geophysics, Geosystems*, 5(5), Q05001. <https://doi.org/10.1029/2004gc000696>

Al-Rousan, S. A., Al-Shloul, R. N., Al-Horani, F. A., & Abu-Hilal, A. H. (2007). Heavy metal contents in growth bands of *Porites* corals: Record of anthropogenic and human developments from the Jordanian Gulf of Aqaba. *Marine Pollution Bulletin*, 54(12), 1912–1922. <https://doi.org/10.1016/j.marpolbul.2007.08.014>

Altschul, S. F., Gish, W., Miller, W., Myers, E. W., & Lipman, D. J. (1990). Basic local alignment search tool. *Journal of Molecular Biology*, 215(3), 403–410. <https://doi.org/10.1006/jmbi.1990.9999>

Amiel, A. J., Friedman, G. M., & Miller, D. S. (1973). Distribution and nature of incorporation of trace elements in modern aragonitic corals. *Sedimentology*, 20(1), 47–64. <https://doi.org/10.1111/j.1365-3091.1973.tb01606.x>

Anthony, K. R. N. (1999). A tank system for studying benthic aquatic organisms at predictable levels of turbidity and sedimentation: Case study examining coral growth. *Limnology and Oceanography*, 44(6), 1415–1422. <https://doi.org/10.4319/lo.1999.44.6.1415>

Anu, G., Kumar, N. C., Jayalakshmi, K. J., & Nair, S. M. (2007). Monitoring of heavy metal partitioning in reef corals of Lakshadweep Archipelago, Indian Ocean. *Environmental Monitoring and Assessment*, 128(1–3), 195–208. <https://doi.org/10.1007/s10661-006-9305-7>

Arumugam, N., Chelliapan, S., Thirugnana, S. T., & Jasni, A. B. (2020). Optimisation of heavy metals uptake from Leachate using red seaweed *Gracilaria changii*. *Journal of Environmental Treatment Techniques*, 8, 1089–1092.

Barakat, S. A., Al-Rousan, S., & Al-Trabeen, M. S. (2015). Use of scleractinian corals to indicate marine pollution in the northern Gulf of Aqaba, Jordan. *Environmental Monitoring and Assessment*, 187(2), 1–12. <https://doi.org/10.1007/s10661-015-4275-2>

Batista, D., Muricy, G., Rocha, R. C., & Mieleky, N. F. (2014). Marine sponges with contrasting life histories can be complementary biomonitors of heavy metal pollution in coastal ecosystems. *Environmental Science and Pollution Research*, 21(9), 5785–5794. <https://doi.org/10.1007/s11356-014-2530-7>

Baudouin, M. F., & Scoppa, P. (1974). Acute toxicity of various metals to freshwater zooplankton. *Bulletin of Environmental Contamination and Toxicology*, 12(6), 745–751. <https://doi.org/10.1007/bf01685925>

Besada, V., Andrade, J. M., Schultze, F., & González, J. J. (2009). Heavy metals in edible seaweeds commercialised for human consumption. *Journal of Marine Systems*, 75(1–2), 305–313. <https://doi.org/10.1016/j.jmarsys.2008.10.010>

Bilings, G. K., & Ragland, P. C. (1968). Geochemistry and mineralogy of the recent reef and lagoonal sediments south of Belize (British Honduras). *Chemical Geology*, 3(2), 135–153. [https://doi.org/10.1016/0009-2541\(68\)90006-5](https://doi.org/10.1016/0009-2541(68)90006-5)

Bjerrum, N. (1936). *Bjerrum's inorganic chemistry* (3rd Danish ed.). Heinemann.

Bosch, A. C., O'Neill, B., Sigge, G. O., Kerwath, S. E., & Hoffman, L. C. (2016). Heavy metals in marine fish meat and consumer health: A review. *Journal of the Science of Food and Agriculture*, 96(1), 32–48. <https://doi.org/10.1002/jsfa.7360>

Brown, B. E., Tudhope, A. W., Le Tissier, M. D. A., & Scoffin, T. P. (1991). A novel mechanism for iron incorporation into coral skeletons. *Coral Reefs*, 10(4), 211–215. <https://doi.org/10.1007/bf00336776>

Byrne, R. H. (2002). Inorganic speciation of dissolved elements in seawater: The influence of pH on concentration ratios. *Geochemical Transactions*, 3(1), 11. <https://doi.org/10.1186/1467-4866-3-11>

Cacciapaglia, C., & van Woesik, R. (2018). Marine species distribution modelling and the effects of genetic isolation under climate change. *Journal of Biogeography*, 45(1), 154–163. <https://doi.org/10.1111/jbi.13115>

Capasso, L., Ganot, P., Planas-Bielsa, V., Tambutté, S., & Zoccola, D. (2021). Intracellular pH regulation: Characterization and functional investigation of H⁺ transporters in *Stylophora pistillata*. *BMC Molecular and Cell Biology*, 22, 1–19. <https://doi.org/10.1186/s12860-021-00353-x>

Carriquiry, J. D., & Horta-Puga, G. (2010). The Ba/Ca record of corals from the Southern Gulf of Mexico: Contributions from land-use changes, fluvial discharge and oil-drilling muds. *Marine Pollution Bulletin*, 60(9), 1625–1630. <https://doi.org/10.1016/j.marpolbul.2010.06.007>

Carriquiry, J. D., & Villaescusa, J. A. (2010). Coral Cd/Ca and Mn/Ca records of ENSO variability in the Gulf of California. *Climate of the Past*, 6(3), 401–410. <https://doi.org/10.5194/cp-6-401-2010>

Cebrian, E., Uriz, M.-J., & Turon, X. (2007). Sponges as biomonitors of heavy metals in spatial and temporal surveys in northwestern Mediterranean: Multispecies comparison. *Environmental Toxicology and Chemistry: An International Journal*, 26(11), 2430–2439. <https://doi.org/10.1897/07-292.1>

Chapman, P. M. (2007). Determining when contamination is pollution — Weight of evidence determinations for sediments and effluents. *Environment International*, 33(4), 492–501. <https://doi.org/10.1016/j.envint.2006.09.001>

Chen, T.-R., Yu, K.-F., Li, S., Price, G. J., Shi, Q., & Wei, G.-J. (2010). Heavy metal pollution recorded in *Porites* corals from Daya Bay, northern South China Sea. *Marine Environmental Research*, 70(3–4), 318–326. <https://doi.org/10.1016/j.marenvres.2010.06.004>

- Clark, T. R., Zhao, J.-X., Feng, Y.-X., Done, T. J., Jupiter, S., Lough, J., & Pandolfi, J. M. (2012). Spatial variability of initial $^{230}\text{Th}/^{232}\text{Th}$ in modern *Porites* from the inshore region of the Great Barrier Reef. *Geochimica et Cosmochimica Acta*, 78, 99–118. <https://doi.org/10.1016/j.gca.2011.11.032>
- Correge, T. (2006). Monitoring of terrestrial input by massive corals. *Journal of Geochemical Exploration*, 88(1–3), 380–383. <https://doi.org/10.1016/j.gexplo.2005.08.080>
- Cuif, J.-P., Dauphin, Y., Berthet, P., & Jegoudez, J. (2004). Associated water and organic compounds in coral skeletons: Quantitative thermogravimetry coupled to infrared absorption spectrometry. *Geochemistry, Geophysics, Geosystems*, 5(11), Q11011. <https://doi.org/10.1029/2004gc000783>
- Cuif, J.-P., Dauphin, Y., Doucet, J., Salome, M., & Susini, J. (2003). XANES mapping of organic sulfate in three scleractinian coral skeletons. *Geochimica et Cosmochimica Acta*, 67(1), 75–83. [https://doi.org/10.1016/s0016-7037\(02\)01041-4](https://doi.org/10.1016/s0016-7037(02)01041-4)
- Cuif, J.-P., Dauphin, Y., & Gautret, P. (1999). Compositional diversity of soluble mineralizing matrices in some recent coral skeletons compared to fine-scale growth structures of fibres: Discussion of consequences for biomineralization and diagenesis. *International Journal of Earth Sciences*, 88(3), 582–592. <https://doi.org/10.1007/s005310050286>
- Dar, M. A. R., Soliman, F. A., & Abd Allah, I. M. (2018). The contributions of flashfloods on the heavy metals incorporations within the coral skeletons at Gulfs of Suez and Aqaba, Egypt. *International Journal of Ecotoxicology and Ecobiology*, 3, 11.
- David, C. P. (2003). Heavy metal concentrations in growth bands of corals: A record of mine tailings input through time (Marinduque Island, Philippines). *Marine Pollution Bulletin*, 46(2), 187–196. [https://doi.org/10.1016/s0025-326x\(02\)00315-6](https://doi.org/10.1016/s0025-326x(02)00315-6)
- Davis, T. A., Volesky, B., & Vieira, R. (2000). *Sargassum* seaweed as biosorbent for heavy metals. *Water Research*, 34(17), 4270–4278. [https://doi.org/10.1016/s0043-1354\(00\)00177-9](https://doi.org/10.1016/s0043-1354(00)00177-9)
- D'Croz, L., Maté, J. L., & Oke, J. E. (2001). Responses to elevated sea water temperature and UV radiation in the coral *Porites lobata* from upwelling and non-upwelling environments on the Pacific coast of Panama. *Bulletin of Marine Science*, 69, 203–214.
- DeLong, K. L., Quinn, T. M., Taylor, F. W., Shen, C.-C., & Lin, K. (2013). Improving coral-base paleoclimate reconstructions by replicating 350 years of coral Sr/Ca variations. *Palaeogeography, Palaeoclimatology, Palaeoecology*, 373, 6–24. <https://doi.org/10.1016/j.palaeo.2012.08.019>
- Diagomanolin, V., Farhang, M., Ghazi-Khansari, M., & Jafarzadeh, N. (2004). Heavy metals (Ni, Cr, Cu) in the Karoon waterway river, Iran. *Toxicology Letters*, 151(1), 63–67. <https://doi.org/10.1016/j.toxlet.2004.02.018>
- Ellwood, M. J. (2004). Zinc and cadmium speciation in subantarctic waters east of New Zealand. *Marine Chemistry*, 87(1–2), 37–58. <https://doi.org/10.1016/j.marchem.2004.01.005>
- El-Sorogy, A. S., Mohamed, M. A., & Nour, H. E. (2012). Heavy metals contamination of the Quaternary coral reefs, Red Sea coast, Egypt. *Environmental Earth Sciences*, 67(3), 777–785. <https://doi.org/10.1007/s12665-012-1535-0>
- Erez, J., & Braun, A. (2007). Calcification in hermatypic corals is based on direct seawater supply to the biomineralisation site. *Geochimica et Cosmochimica Acta*, 71(15), SA260.
- Esslemont, G. (2000). Heavy metals in seawater, marine sediments and corals from the Townsville section, Great Barrier Reef Marine Park, Queensland. *Marine Chemistry*, 71(3–4), 215–231. [https://doi.org/10.1016/s0304-4203\(00\)00050-5](https://doi.org/10.1016/s0304-4203(00)00050-5)
- Farkaš, J., Frýda, J., Paulukat, C., Hathorne, E. C., Matoušková, Š., Rohovec, J., et al. (2018). Chromium isotope fractionation between modern seawater and biogenic carbonates from the Great Barrier Reef, Australia: Implications for the paleo-seawater $\delta^{53}\text{Cr}$ reconstruction. *Earth and Planetary Science Letters*, 498, 140–151. <https://doi.org/10.1016/j.epsl.2018.06.032>
- Finch, A. A., & Allison, N. (2008). Mg structural state in coral aragonite and implications for the paleoenvironmental proxy. *Geophysical Research Letters*, 35(8), L08704. <https://doi.org/10.1029/2008gl033543>
- Fleitmann, D., Dunbar, R. B., McCulloch, M., Mudelsee, M., Vuille, M., McClanahan, T. R., et al. (2007). East African soil erosion recorded in a 300 year old coral colony from Kenya. *Geophysical Research Letters*, 34(4), L04401. <https://doi.org/10.1029/2006gl028525>
- Forsman, Z. H., Barshis, D. J., Hunter, C. L., & Toonen, R. J. (2009). Shape-shifting corals: Molecular markers show morphology is evolutionarily plastic in *Porites*. *BMC Evolutionary Biology*, 9, 1–9. <https://doi.org/10.1186/1471-2148-9-45>
- Fricker, M. B., Kutscher, D., Aeschlimann, B., Frommer, J., Dietiker, R., Bettmer, J., & Günther, D. (2011). High spatial resolution trace element analysis by LA-ICP-MS using a novel ablation cell for multiple or large samples. *International Journal of Mass Spectrometry*, 307(1–3), 39–45. <https://doi.org/10.1016/j.ijms.2011.01.008>
- Frontalini, F., & Coccioni, R. (2008). Benthic foraminifera for heavy metal pollution monitoring: A case study from the central Adriatic Sea coast of Italy. *Estuarine, Coastal and Shelf Science*, 76(2), 404–417. <https://doi.org/10.1016/j.ecss.2007.07.024>
- Gagnon, A. C., Adkins, J. F., & Erez, J. (2012). Seawater transport during coral biomineralization. *Earth and Planetary Science Letters*, 329, 150–161. <https://doi.org/10.1016/j.epsl.2012.03.005>
- Garbe-Schönberg, D., & Müller, S. (2014). Nano-particulate pressed powder tablets for LA-ICP-MS. *Journal of Analytical Atomic Spectrometry*, 29(6), 990–1000. <https://doi.org/10.1039/c4ja00007b>
- Green, D. H., Edmunds, P. J., & Carpenter, R. C. (2008). Increasing relative abundance of *Porites astreoides* on Caribbean reefs mediated by an overall decline in coral cover. *Marine Ecology Progress Series*, 359, 1–10. <https://doi.org/10.3354/meps07454>
- Hammer, Ø., Harper, D. A. T., & Ryan, P. D. (2001). PAST: Paleontological statistics software package for education and data analysis. *Palaeontologia Electronica*, 4, 9.
- Hanna, R. G., & Muir, G. L. (1990). Red Sea corals as biomonitors of trace metal pollution. *Environmental Monitoring and Assessment*, 14(2–3), 211–222. <https://doi.org/10.1007/bf00677917>
- Hirose, K. (2006). Chemical speciation of trace metals in seawater: A review. *Analytical Sciences*, 22(8), 1055–1063. <https://doi.org/10.2116/analsci.22.1055>
- Hurlbert, S. H. (1984). Pseudoreplication and the design of ecological field experiments. *Ecological Monographs*, 54(2), 187–211. <https://doi.org/10.2307/1942661>
- Inoue, M., Nohara, M., Okai, T., Suzuki, A., & Kawahata, H. (2004). Concentrations of trace elements in carbonate reference materials coral JCP-1 and giant clam JCT-1 by inductively coupled plasma-mass spectrometry. *Geostandards and Geoanalytical Research*, 28(3), 411–416. <https://doi.org/10.1111/j.1751-908x.2004.tb00759.x>
- Jafarabadi, A. R., Bakhtiari, A. R., Maisano, M., Pereira, P., & Cappello, T. (2018). First record of bioaccumulation and bioconcentration of metals in Scleractinian corals and their algal symbionts from Kharg and Lark coral reefs (Persian Gulf, Iran). *Science of the Total Environment*, 640, 1500–1511.
- Jeremiason, J. D., Portner, J. C., Aiken, G. R., Hiranaka, A. J., Dvorak, M. T., Tran, K. T., & Latch, D. E. (2015). Photoreduction of Hg(II) and photodemethylation of methylmercury: The key role of thiol sites on dissolved organic matter. *Environmental Science: Processes & Impacts*, 17(11), 1892–1903. <https://doi.org/10.1039/C5EM00305A>

- Jiang, W., Yu, K., Wang, N., Yang, H., Yang, H., Xu, S., et al. (2020). Distribution coefficients of trace metals between modern coral-lattices and seawater in the northern South China Sea: Species and SST dependencies. *Journal of Asian Earth Sciences*, 187, 104082. <https://doi.org/10.1016/j.jseas.2019.104082>
- Jochum, K. P., Garbe-Schönberg, D., Vetter, M., Stoll, B., Weis, U., Weber, M., et al. (2019). Nano-powdered calcium carbonate reference materials: Significant progress for microanalysis? *Geostandards and Geoanalytical Research*, 43(4), 595–609. <https://doi.org/10.1111/ggr.12292>
- Jochum, K. P., Weis, U., Stoll, B., Kuzmin, D., Yang, Q., Raczek, I., et al. (2011). Determination of reference values for NIST SRM 610–617 glasses following ISO guidelines. *Geostandards and Geoanalytical Research*, 35(4), 397–429. <https://doi.org/10.1111/j.1751-908x.2011.00120.x>
- Kaczmarczyk, L., & Richardson, L. L. (2007). Transmission of growth anomalies between Indo-Pacific *Porites* corals. *Journal of Invertebrate Pathology*, 94(3), 218–221. <https://doi.org/10.1016/j.jip.2006.11.007>
- Kato, K., Misawa, K., Kuma, K.-i., & Miyata, T. (2002). MAFFT: A novel method for rapid multiple sequence alignment based on fast Fourier transform. *Nucleic Acids Research*, 30(14), 3059–3066. <https://doi.org/10.1093/nar/gk436>
- Kato, K., & Standley, D. M. (2013). MAFFT multiple sequence alignment software version 7: Improvements in performance and usability. *Molecular Biology and Evolution*, 30(4), 772–780. <https://doi.org/10.1093/molbev/mst010>
- Kefu, Y., Tegu, C., Dingcheng, H., Huanting, Z., Jinliang, Z., & Dongsheng, L. (2001). The high-resolution climate recorded in the $\delta^{18}\text{O}$ of *Porites lutea* from the Nansha Islands of China. *Chinese Science Bulletin*, 46(24), 2097–2102. <https://doi.org/10.1007/bf02901141>
- Kojima, A. C., Thompson, D. M., Hlohowskyj, S. R., Carilli, J. E., Gordon, G., Goepfert, T. J., et al. (2022). A mechanistic investigation of the coral Mn/Ca-based trade-wind proxy at Kiritimati. *Geochimica et Cosmochimica Acta*, 328, 58–75. <https://doi.org/10.1016/j.gca.2022.04.030>
- Kotow, S., & Pällike, H. (2018). QAnlySeries—a cross-platform time series tuning and analysis tool. In *AGU Fall Meeting Abstracts* (Vol. 2018).
- Kourandeh, M. B., Nabavi, S. M. B., Shokri, M. R., Ghanemi, K., & Feng, Y. (2021). Trace metal content in annually banded scleractinian coral *Porites lobata* across the northern Persian Gulf. *Environmental Science and Pollution Research*, 1–13.
- Lamborg, C. H., Swarr, G., Hughen, K., Jones, R. J., Birdwhistell, S., Furby, K., et al. (2013). Determination of low-level mercury in coralline aragonite by calcination-isotope dilution-inductively coupled plasma-mass spectrometry and its application to Diploria specimens from Castle Harbour, Bermuda. *Geochimica et Cosmochimica Acta*, 109, 27–37. <https://doi.org/10.1016/j.gca.2013.01.026>
- Larocque, A. C. L., & Rasmussen, P. E. (1998). An overview of trace metals in the environment, from mobilization to remediation. *Environmental Geology*, 33(2–3), 85–91. <https://doi.org/10.1007/s002540050227>
- Leonard, N. D., Welsh, K. J., Nguyen, A. D., Sadler, J., Pandolfi, J. M., Clark, T. R., et al. (2019). High resolution geochemical analysis of massive *Porites* spp. corals from the Wet Tropics, Great Barrier Reef: Rare earth elements, yttrium and barium as indicators of terrigenous input. *Marine Pollution Bulletin*, 149, 110634. <https://doi.org/10.1016/j.marpolbul.2019.110634>
- Lewis, S. E., Brodie, J. E., McCulloch, M. T., Mallela, J., Jupiter, S. D., Williams, H. S., et al. (2012). An assessment of an environmental gradient using coral geochemical records, Whitsunday Islands, Great Barrier Reef, Australia. *Marine Pollution Bulletin*, 65(4–9), 306–319. <https://doi.org/10.1016/j.marpolbul.2011.09.030>
- Li, T., Cai, G., Zhang, M., Li, S., & Nie, X. (2021). The response of benthic foraminifera to heavy metals and grain sizes: A case study from Hainan Island, China. *Marine Pollution Bulletin*, 167, 112328. <https://doi.org/10.1016/j.marpolbul.2021.112328>
- Linn, L. J., Delaney, M. L., & Druffel, E. R. M. (1990). Trace metals in contemporary and seventeenth-century Galapagos coral: Records of seasonal and annual variations. *Geochimica et Cosmochimica Acta*, 54(2), 387–394. [https://doi.org/10.1016/0016-7037\(90\)90327-h](https://doi.org/10.1016/0016-7037(90)90327-h)
- Liu, Q., Wang, F., Meng, F., Jiang, L., Li, G., & Zhou, R. (2018). Assessment of metal contamination in estuarine surface sediments from Dongying City, China: Use of a modified ecological risk index. *Marine Pollution Bulletin*, 126, 293–303. <https://doi.org/10.1016/j.marpolbul.2017.11.017>
- Lord, K. S., Barcala, A., Aichelman, H. E., Kriefall, N. G., Brown, C., Knasin, L., et al. (2021). Distinct phenotypes associated with mangrove and lagoon habitats in two widespread Caribbean corals, *Porites astreoides* and *Porites divaricata*. *The Biological Bulletin*, 240(3), 0–190. <https://doi.org/10.1086/714047>
- Lough, J. M., Barnes, D. J., & Taylor, R. B. (1996). The potential of massive corals for the study of high-resolution climate variation in the past millennium. In *Climatic variations and forcing mechanisms of the last 2000 years* (pp. 355–371). Springer.
- Lu, Y., Gao, X., & Chen, C.-T. A. (2019). Separation and determination of colloidal trace metals in seawater by cross-flow ultrafiltration, liquid-liquid extraction and ICP-MS. *Marine Chemistry*, 215, 103685. <https://doi.org/10.1016/j.marchem.2019.103685>
- Mansour, A. M., Askalany, M. S., Madkour, H. A., & Assran, B. B. (2013). Assessment and comparison of heavy-metal concentrations in marine sediments in view of tourism activities in Hurghada area, northern Red Sea, Egypt. *The Egyptian Journal of Aquatic Research*, 39(2), 91–103. <https://doi.org/10.1016/j.ejar.2013.07.004>
- Mass, T., Drake, J. L., Heddleston, J. M., & Falkowski, P. G. (2017). Nanoscale visualization of biomineral formation in coral proto-polyps. *Current Biology*, 27(20), 3191–3196.e3. <https://doi.org/10.1016/j.cub.2017.09.012>
- McCulloch, M., Fallon, S., Wyndham, T., Hendy, E., Lough, J., & Barnes, D. (2003). Coral record of increased sediment flux to the inner Great Barrier Reef since European settlement. *Nature*, 421(6924), 727–730. <https://doi.org/10.1038/nature01361>
- Mieremet, B. (1997). *Report of the Middle East Seas Regional Strategy Workshop for the International Coral Reef Initiative: Aqaba, Jordan, 21–25 September 1997*. Office of Oceanic and Coastal Resources Management, National Ocean and Atmospheric Administration.
- Miller, L. A., & Bruland, K. W. (1995). Organic speciation of silver in marine waters. *Environmental Science & Technology*, 29(10), 2616–2621. <https://doi.org/10.1021/es00010a024>
- Mohammed, T. A.-A. A., & Dar, M. A. (2010). Ability of corals to accumulate heavy metals, Northern Red Sea, Egypt. *Environmental Earth Sciences*, 59(7), 1525–1534. <https://doi.org/10.1007/s12665-009-0138-x>
- Munsell, D., Kramar, U., Dissard, D., Nehrke, G., Berner, Z., Bijma, J., et al. (2010). Heavy metal incorporation in foraminiferal calcite: Results from multi-element enrichment culture experiments with *Ammonia tepida*. *Biogeosciences*, 7(8), 2339–2350. <https://doi.org/10.5194/bg-7-2339-2010>
- Nardelli, M. P., Malferrari, D., Ferretti, A., Bartolini, A., Sabbatini, A., & Negri, A. (2016). Zinc incorporation in the miliolid foraminifer *Pseudotriloculina rotunda* under laboratory conditions. *Marine Micropaleontology*, 126, 42–49. <https://doi.org/10.1016/j.marmicro.2016.06.001>
- Nguyen, A. D., Zhao, J. X., Feng, Y. X., Hu, W. P., Yu, K. F., Gasparon, M., et al. (2013). Impact of recent coastal development and human activities on Nha Trang Bay, Vietnam: Evidence from a *Porites lutea* geochemical record. *Coral Reefs*, 32(1), 181–193. <https://doi.org/10.1007/s00338-012-0962-4>
- Nguyen, L.-T., Schmidt, H. A., von Haeseler, A., & Minh, B. Q. (2015). IQ-TREE: A fast and effective stochastic algorithm for estimating maximum-likelihood phylogenies. *Molecular Biology and Evolution*, 32(1), 268–274. <https://doi.org/10.1093/molbev/msu300>

- Nour, H. E. S. (2019). Assessment of heavy metals contamination in surface sediments of Sabratha, Northwest Libya. *Arabian Journal of Geosciences*, 12(6), 1–9. <https://doi.org/10.1007/s12517-019-4343-y>
- Nour, H. E. S., & Nour, E. S. (2020). Using coral skeletons for monitoring of heavy metals pollution in the Red Sea Coast, Egypt. *Arabian Journal of Geosciences*, 13(10), 1–12. <https://doi.org/10.1007/s12517-020-05308-8>
- Oldham, V. E., Lamborg, C. H., & Hansel, C. M. (2020). The spatial and temporal variability of Mn speciation in the coastal Northwest Atlantic Ocean. *Journal of Geophysical Research: Oceans*, 125(1), e2019JC015167. <https://doi.org/10.1029/2019JC015167>
- Oron, S., Sadekov, A., Katz, T., & Goodman-Tchernov, B. (2021). Benthic foraminifera geochemistry as a monitoring tool for heavy metal and phosphorus pollution—A post fish-farm removal case study. *Marine Pollution Bulletin*, 168, 112443. <https://doi.org/10.1016/j.marpolbul.2021.112443>
- Prouty, N. G., Field, M. E., Stock, J. D., Jupiter, S. D., & McCulloch, M. (2010). Coral Ba/Ca records of sediment input to the fringing reef of the southshore of Moloka'i, Hawai'i over the last several decades. *Marine Pollution Bulletin*, 60(10), 1822–1835. <https://doi.org/10.1016/j.marpolbul.2010.05.024>
- Prouty, N. G., Hughen, K. A., & Carilli, J. (2008). Geochemical signature of land-based activities in Caribbean coral surface samples. *Coral Reefs*, 27(4), 727–742. <https://doi.org/10.1007/s00338-008-0413-4>
- Readman, J. W., Tolosa, I., Law, A. T., Bartocci, J., Azemard, S., Hamilton, T., et al. (1996). Discrete bands of petroleum hydrocarbons and molecular organic markers identified within massive coral skeletons. *Marine Pollution Bulletin*, 32(5), 437–443. [https://doi.org/10.1016/0025-326x\(96\)83974-9](https://doi.org/10.1016/0025-326x(96)83974-9)
- Reichelt-Brushett, A. J., & Harrison, P. L. (2005). The effect of selected trace metals on the fertilization success of several scleractinian coral species. *Coral Reefs*, 24(4), 524–534. <https://doi.org/10.1007/s00338-005-0013-5>
- Reichelt-Brushett, A. J., & McOrist, G. (2003). Trace metals in the living and nonliving components of scleractinian corals. *Marine Pollution Bulletin*, 46(12), 1573–1582. [https://doi.org/10.1016/S0025-326X\(03\)00323-0](https://doi.org/10.1016/S0025-326X(03)00323-0)
- Reyes-Bonilla, H. (1992). New records for hermatypic corals (Anthozoa Scleractinia) in the Gulf of California, Mexico, with an historical and biogeographical discussion. *Journal of Natural History*, 26(6), 1163–1175. <https://doi.org/10.1080/00222939200770671>
- Rodríguez, G. R., & Morales, E. O. (2020). Assessment of heavy metal contamination at Tallaboa Bay (Puerto Rico) by marine sponges' bioaccumulation and fungal community composition. *Marine Pollution Bulletin*, 161, 111803. <https://doi.org/10.1016/j.marpolbul.2020.111803>
- Saha, N., Webb, G. E., & Zhao, J.-X. (2016). Coral skeletal geochemistry as a monitor of inshore water quality. *Science of the Total Environment*, 566, 652–684. <https://doi.org/10.1016/j.scitotenv.2016.05.066>
- Santhanam, P. (2011). An investigation on heavy metals accumulation in water, sediment and small marine food chain (plankton and fish) from Coromandel Coast, Southeast Coast of India. *Indian Journal Of Natural Sciences International Bimonthly ISSN*, 976, 997.
- Sayani, H. R., Thompson, D. M., Carilli, J. E., Marchitto, T. M., Chapman, A. U., & Cobb, K. M. (2021). Reproducibility of coral Mn/Ca-based wind reconstructions at Kiritimati Island and Butaritari Atoll. *Geochemistry, Geophysics, Geosystems*, 22(3), e2020GC009398. <https://doi.org/10.1029/2020GC009398>
- Sayers, E. W., Barrett, T., Benson, D. A., Bryant, S. H., Canese, K., Chetvernin, V., et al. (2009). Database resources of the National Center for Biotechnology Information. *Nucleic Acids Research*, 39, D38–D51. <https://doi.org/10.1093/nar/gkq1172>
- Schmidt, S. (2024). Time resolved trace element-to-calcium values measured with Laser ablation ICP-MS along lines of coral colony A to D (*Porites lobata* and *Porites lichen*) cultured with different metal concentrations [Dataset]. *PANGAEA*. <https://doi.org/10.1594/PANGAEA.938748>
- Schmidt, S., Hathorne, E. C., Schönfeld, J., & Garbe-Schönberg, D. (2022). Heavy metal uptake of nearshore benthic foraminifera during multi-metal culturing experiments. *Biogeosciences*, 19(3), 629–664. <https://doi.org/10.5194/bg-19-629-2022>
- Schneider, R. C., & Smith, S. V. (1982). Skeletal Sr content and density in *Porites* spp. in relation to environmental factors. *Marine Biology*, 66(2), 121–131. <https://doi.org/10.1007/bf00397185>
- Séré, M. G., Schleyer, M. H., Quod, J. P., & Chabanet, P. (2012). *Porites* white patch syndrome: An unreported coral disease on Western Indian Ocean reefs. *Coral Reefs*, 31(3), 739. <https://doi.org/10.1007/s00338-012-0897-9>
- Shen, G. T. (1996). Rapid changes in the tropical ocean and the use of corals as monitoring systems. In A. Berger (Ed.), *Geoindicator: Assessing rapid environmental changes in earth systems* (pp. 125–169). Brookfield.
- Shen, G. T., & Boyle, E. A. (1988). Determination of lead, cadmium and other trace metals in annually-banded corals. *Chemical Geology*, 67(1–2), 47–62. [https://doi.org/10.1016/0009-2541\(88\)90005-8](https://doi.org/10.1016/0009-2541(88)90005-8)
- Shen, G. T., Campbell, T. M., Dunbar, R. B., Wellington, G. M., Colgan, M. W., & Glynn, P. W. (1991). Paleochemistry of manganese in corals from the Galapagos Islands. *Coral Reefs*, 10(2), 91–100. <https://doi.org/10.1007/bf00571827>
- Sonone, S. S., Jadhav, S., Sankhla, M. S., & Kumar, R. (2020). Water contamination by heavy metals and their toxic effect on aquaculture and human health through food Chain. *Letters in Applied NanoBioScience*, 10, 2148–2166.
- Sowa, K., Watanabe, T., Kan, H., & Yamano, H. (2014). Influence of land development on Holocene *Porites* coral calcification at Nagura Bay, Ishigaki Island, Japan. *PLoS One*, 9(2), e88790. <https://doi.org/10.1371/journal.pone.0088790>
- St John, B. (1974). Heavy metals in the skeletal carbonate of scleractinian corals. In *Proceedings of 2nd International Coral Reef Symposium* (pp. 461–469).
- Sun, C.-Y., Stiffler, C. A., Chopdekar, R. V., Schmidt, C. A., Parida, G., Schoeppler, V., et al. (2020). From particle attachment to space-filling coral skeletons. *Proceedings of the National Academy of Sciences*, 117(48), 30159–30170. <https://doi.org/10.1073/pnas.2012025117>
- Sun, R., Hintelmann, H., Liu, Y., Li, X., & Dimock, B. (2016). Two centuries of coral skeletons from the northern South China Sea record mercury emissions from modern Chinese wars. *Environmental Science & Technology*, 50(11), 5481–5488. <https://doi.org/10.1021/acs.est.5b05965>
- Tambutté, S., Holcomb, M., Ferrier-Pagès, C., Reynaud, S., Tambutté, É., Zoccola, D., & Allemand, D. (2011). Coral biomineralization: From the gene to the environment. *Journal of Experimental Marine Biology and Ecology*, 408(1–2), 58–78. <https://doi.org/10.1016/j.jembe.2011.07.026>
- Taubner, I., Böhm, F., Eisenhauer, A., Tambutté, E., Tambutté, S., Moldzio, S., & Bleich, M. (2017). An improved approach investigating epithelial ion transport in scleractinian corals. *Limnology and Oceanography: Methods*, 15(9), 753–765. <https://doi.org/10.1002/lom3.10194>
- Thornton, I. (1995). *Metals in the global environment: Facts and misconceptions*. International Council on Metals and the Environment.
- Tisthammer, K. H., & Richmond, R. H. (2018). Corallite skeletal morphological variation in Hawaiian *Porites lobata*. *Coral Reefs*, 37(2), 445–456. <https://doi.org/10.1007/s00338-018-1670-5>
- Titelboim, D., Sadekov, A., Blumenfeld, M., Almogi-Labin, A., Herut, B., Halicz, L., et al. (2021). Monitoring of heavy metals in seawater using single chamber foraminiferal sclerochronology. *Ecological Indicators*, 120, 106931. <https://doi.org/10.1016/j.ecolind.2020.106931>
- Tortolero-Langarica, J. J. A., Carricart-Ganivet, J. P., Cupul-Magaña, A. L., & Rodríguez-Troncoso, A. P. (2017). Historical insights on growth rates of the reef-building corals *Pavona gigantea* and *Porites panamensis* from the Northeastern tropical Pacific. *Marine Environmental Research*, 132, 23–32. <https://doi.org/10.1016/j.marenvres.2017.10.004>

- Valverde, F., Costas, M., Pena, F., Lavilla, I., & Bendicho, C. (2008). Determination of total silver and silver species in coastal seawater by inductively-coupled plasma mass spectrometry after batch sorption experiments with Chelex-100 resin. *Chemical Speciation and Bioavailability*, 20(4), 217–226. <https://doi.org/10.3184/095422908X381306>
- Venugopal, B., & Luckey, T. D. (1975). Toxicology of nonradio-active heavy metals and their salts. In T. D. Luckey, B. Venugopal, & D. Hutcheson (Eds.), *Heavy metal toxicity, safety and hormology*. George Thieme.
- Weis, J. S. (2015). *Marine pollution: What everyone needs to know* (p. 273). Oxford University Press.
- Williams, T. M., Rees, J. G., & Setiapermana, D. (2000). Metals and trace organic compounds in sediments and waters of Jakarta Bay and the Pulau Seribu Complex, Indonesia. *Marine Pollution Bulletin*, 40(3), 277–285. [https://doi.org/10.1016/s0025-326x\(99\)00226-x](https://doi.org/10.1016/s0025-326x(99)00226-x)
- Wu, Y., Fallon, S. J., Cantin, N. E., & Lough, J. M. (2021). Surface ocean radiocarbon from a *Porites* coral record in the Great Barrier Reef: 1945–2017. *Radiocarbon*, 63(4), 1–11. <https://doi.org/10.1017/rdc.2020.141>
- Zhang, J., & Gao, X. (2015). Heavy metals in surface sediments of the intertidal Laizhou Bay, Bohai Sea, China: Distributions, sources and contamination assessment. *Marine Pollution Bulletin*, 98(1–2), 320–327. <https://doi.org/10.1016/j.marpolbul.2015.06.035>
- Zhong, S., & Mucci, A. (1995). Partitioning of rare earth elements (REEs) between calcite and seawater solutions at 25°C and 1 atm, and high dissolved REE concentrations. *Geochimica et Cosmochimica Acta*, 59(3), 443–453. [https://doi.org/10.1016/0016-7037\(94\)00381-U](https://doi.org/10.1016/0016-7037(94)00381-U)

References From the Supporting Information

- Cooper, T. F., De'Ath, G., Fabricius, K. E., & Lough, J. M. (2008). Declining coral calcification in massive *Porites* in two nearshore regions of the northern Great Barrier Reef. *Global Change Biology*, 14(3), 529–538. <https://doi.org/10.1111/j.1365-2486.2007.01520.x>
- Edinger, E. N., & Risk, M. J. (2000). Effect of land-based pollution on central Java coral reefs. *Journal of Coastal Development*, 3, 593–613.
- Fallon, S. J., McCulloch, M. T., van Woesik, R., & Sinclair, D. J. (1999). Corals at their latitudinal limits: Laser ablation trace element systematics in *Porites* from Shirigai Bay, Japan. *Earth and Planetary Science Letters*, 172(3–4), 221–238. [https://doi.org/10.1016/s0012-821x\(99\)00200-9](https://doi.org/10.1016/s0012-821x(99)00200-9)
- Grottoli, A. G., Matthews, K. A., Palardy, J. E., & McDonough, W. F. (2013). High resolution coral Cd measurements using LA-ICP-MS and ID-ICP-MS: Calibration and interpretation. *Chemical Geology*, 356, 151–159. <https://doi.org/10.1016/j.chemgeo.2013.08.024>
- Guzman, H. M., & Cortes, J. (1989). Growth rates of eight species of scleractinian corals in the eastern Pacific (Costa Rica). *Bulletin of Marine Science*, 44, 1186–1194.
- Klein, R., & Loya, Y. (1991). Skeletal growth and density patterns of two *Porites* corals from the Gulf of Eilat, Red Sea. *Marine Ecology Progress Series*, 77, 253–259. <https://doi.org/10.3354/meps077253>
- Livingston, H. D., & Thompson, G. (1971). Trace Element concentration in some modern corals. *Limnology and Oceanography*, 16(5), 786–796. <https://doi.org/10.4319/lo.1971.16.5.0786>
- Lough, J. M., Barnes, D. J., Devereux, M. J., Tobin, B. J., & Tobin, S. (1999). *Variability in growth characteristics of massive Porites on the Great Barrier Reef. CRC Reef Research Technical Report* (Vol. 28). Australian Institute of Marine Science.
- Mokhtar, M. B., Praveena, S. M., Aris, A. Z., Yong, O. C., & Lim, A. P. (2012). Trace metal (Cd, Cu, Fe, Mn, Ni and Zn) accumulation in Scleractinian corals: A record for Sabah, Borneo. *Marine Pollution Bulletin*, 64(11), 2556–2563. <https://doi.org/10.1016/j.marpolbul.2012.07.030>
- Shen, G. T. (1986). *Lead and cadmium geochemistry of corals: Reconstruction of historic perturbations in the upper ocean*. Massachusetts Institute of Technology.
- Shen, G. T., & Sanford, C. L. (1990). Trace element indicators of climate variability in reef-building corals. In *Elsevier oceanography series* (pp. 255–283). Elsevier.
- Smith, L. W., Barshis, D., & Birkeland, C. (2007). Phenotypic plasticity for skeletal growth, density and calcification of *Porites lobata* in response to habitat type. *Coral Reefs*, 26(3), 559–567. <https://doi.org/10.1007/s00338-007-0216-z>
- Tortolero-Langarica, J. J. A., Rodríguez-Troncoso, A. P., Carricart-Ganivet, J. P., & Cupul-Magaña, A. L. (2016). Skeletal extension, density and calcification rates of massive free-living coral *Porites lobata* Dana, 1846. *Journal of Experimental Marine Biology and Ecology*, 478, 68–76. <https://doi.org/10.1016/j.jembe.2016.02.005>
- Veeh, H. H., & Turekian, K. K. (1968). Cobalt, silver, and uranium concentrations of reef-building corals in the Pacific Ocean. *Limnology and Oceanography*, 13(2), 304–308. <https://doi.org/10.4319/lo.1968.13.2.0304>
- Yeghicheyan, D., Aubert, D., Bouhnik-le Coz, M., Chmeleff, J., Delpoux, S., Djouaev, I., et al. (2019). A new interlaboratory characterisation of silicon, rare earth elements and twenty-two other trace element concentrations in the natural river water certified reference material SLRS-6 (NRC-CNRC). *Geostandards and Geoanalytical Research*, 43(3), 475–496. <https://doi.org/10.1111/ggr.12268>